INTEGRATION OF PLANAR CIRCUIT ANALYSIS

INTO A

MICROWAVE CIRCUIT DESIGN SOFTWARE

A Thesis Submitted
in Partial Fulfillment of the Requirement
for the Degree of
MASTER OF TECHNOLOGY

by

MAJOR SHARAD SHUKLA

to the

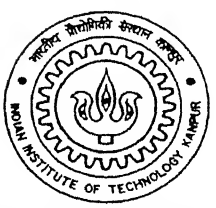

DEPARTMENT OF ELECTRICAL ENGINEERING
INDIAN INSTITUTE OF TECHNOLOGY, KANPUR

JANUARY, 2002

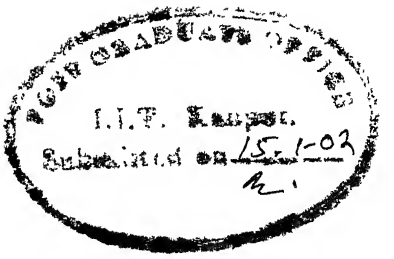

CERTIFICATE

It is certified that the work contained in the thesis entitled " **INTEGRATION OF PLANAR CIRCUIT ANALYSIS INTO A MICROWAVE CIRCUIT DESIGN SOFTWARE** ", by Major Sharad Shukla, has been carried out under my supervision and this work has not been submitted elsewhere for a degree.

Dr. M. Sachidananda

Professor

Department of Electrical Engineering,

Indian Institute of Technology, Kanpur.

15 January, 2002

Abstract

There are a number of commercially available software, which can be used for the design, and analysis of microwave circuits. But their high costs, copyright restrictions and training requirements restrict their utility in the academic environment, as the requirement for the students is to understand the approach and theory behind the development of such a software. Hence, the possibility of developing a simple Graphical User Interface software for microwave circuit design is explored. The basic framework of the software is such that it can integrate different computational techniques available for the analysis of microwave circuit design. As a test case for integration of computational technique, planar circuit analysis is integrated into the software. Planar circuit analysis provides a method for modeling of microwave circuit elements as a 2-dimensional circuit, which is based on the assumption that E-field component is present only in one direction, and hence there is no wave propagation in that direction. By the formulation of planar circuit modeling 2-dimensional wave equation can be solved for the E-field under given boundary conditions. The Green's function approach is used to find the Z-matrix elements for various ports on the periphery of the planar circuit element of simple geometry. Z-matrices are converted into S-matrix elements for characterisation of the microwave circuit. Further Green's function approach has been extended with the use of segmentation and desegmentation to account for complicated geometry of microwave circuit element. Combination of the aforesaid approaches is used for the analysis of three planar structure, rectangular resonator, single step and double step discontinuity for a frequency range from 0.01 to 15 GHz. The substrate Rexolite 1422 type III $\varepsilon_r = 2.53$ is considered in the analysis of the examples. The waveguide model is used to calculate the frequency dependent effective width $w_{eff}(f)$ and $\varepsilon_{eff}(f)$ for accurate characterisation over the desired frequency range.

To my wife, Preeti

ACKNOWLEDGEMENTS

I would like to take this opportunity to attribute successful completion of this thesis to my guide, Dr M. Sachidananda, for not only proposing the thesis topic but also providing me sufficient time whenever I approached him, keeping aside his other work. He has been helpful in channeling my thought process and knowledge in correct directions. He has been a true guide in the sense that he provided me sufficient time to build up my theoretical knowledge and freedom in the choice of computational technique.

I would also like to thank my colleagues Maj. Rajendra Negi, Ashesh, Gangadhar and Subrata for providing useful suggestions, moral support, informative and joyful company during the course of thesis preparation.

I would also like to thank the Department of Electrical Engineering and Advanced Centre for Electronic Systems for all the facilities extended to me and for a cordial working environment.

My sincere thanks to Indian Army, especially Corps of Signals for selecting and sending me to this wonderful institute to achieve this professional degree.

Finally, I would like to lay the major part of my success on the shoulders of my parents, wife and children, for they sacrificed the time due for them in my quest of knowledge. They have been most helpful and understanding through out the course duration.

Contents

List of Figures

Glossary of Symbols

Abbreviations

CAD	Computer Aided Design.
FTD	Finite Time Domain.
GUI	Graphical User Interface.
MIC	Microwave Integrated Circuitry.
PCA	Planar-Circuit Approach.

Symbols

$2d$	Thickness of the dielectric stripline.
h	Thickness of the dielectric microstrip.
w	Width of the port.
f	Frequency.
ω	Angular frequency.
λ	Wavelength.
K_o	Free space propagation constant.
β	Phase constant.
ε	Electric permittivity.
μ	Magnetic permeability.
ε_r	Relative dielectric constant.
v , i	Instantaneous voltage and current.
E,H	Electric and magnetic field vectors.
J	Current density vector.

G	Green's function.
Z	Impedance Matrix.
Y	Admittance Matrix.
S	Scattering parameter matrix.
C	Capacitance.
L	Inductance.
x,y,z	Directions of Cartesian co-ordinate system.
n,s	Normal and tangential direction.

Legend

Subscript n,s,x,y,z	Denotes vector along corresponding direction.
^ over direction	Unit vector along corresponding direction.
Bold face letters	Denotes a vector quantity.

CHAPTER 1

INTRODUCTION

1.1 Introduction

At microwave and millimeter wave frequencies the circuits are essentially distributed type, using transmission line sections as circuit elements. Further even the stray effects of the discontinuities at the junctions or open end of transmission line cannot be ignored, because the performance of the circuit is significantly affected by the stray parameters. Thus, there is a need for accurately evaluating every possible effect while designing a microwave and millimeter wave circuits, and the only way this can be done is by field computations. The fields of the transmission line, discontinuity, junction etc are computed by solving Maxwell's equations along with the boundary conditions to be satisfied at the boundaries of the structure. The equivalent circuit parameters are derived from the **E** & **H** field distributions.

In general, field computation is a time consuming job requiring extensive numerical and analytical work. With the availability of fast computers, several numerical techniques have been developed to solve field problems. Still, the computational time required for characterizing a simple structure like a junction between two dissimilar width transmission lines is significant. It is not convenient in a practical microwave circuit design to start solving the Maxwell's equations to get the field distributions, and then the circuit parameters. Instead, the approach is to characterize each type of discontinuity separately using the field solution, over a wide band of frequencies, and then generate a database of design data or derive empirical relationships to directly obtain lumped circuit equivalent of any structure from the dimensions of the structure. Thus, the computer aided microwave design (CAD) softwares mostly contain these empirical relationships or design databases incorporated into them. There is no commercial microwave CAD software that does the field analysis. The field analysis softwares are developed separately, and are not made the part of the CAD program. This is also necessitated by the variety of circuits and analysis procedures typically applicable for each circuit. No single method can be

used for all types of circuits.

One such analysis procedure is the planar circuit approach (PCA) applicable to a class of microwave circuit patterns realised using printed circuit technology. These are called planar circuits because one of the dimensions is very small compared to wavelength, typically less than 0.1 λ. Under this condition it is assumed that the **E** field has a component only along this dimension, thus reducing the problem of field computation to a 2-dimensional problem, instead of 3-dimensional one. This significantly simplifies the field computation. However, it is important to note that at the edges of the conductor patterns of a planar circuit, there is a fringing **E** field component in the other two dimensions as well. This fact can generally be taken into account by a correction term to the dimension of the circuit, and defined as an equivalent size This size extension takes care of the fringing field contribution. The most important fact to note is that there is no propagation in the dimension along which the size is very small compared to wavelength, which is the basis of a 2-dimensional wave equation formulation.

One important advantage of PCA is that it can analyse arbitrary shaped planar structure and obtain its characteristics. In this thesis we envisage an integration of this method into a CAD program so that it can be used as a design tool, or to generate design database for any other microwave circuit design software. While development of a complete software of this kind is not possible in the short duration of one semester, this thus forms one significant part of the overall software that is envisaged. With the incorporation of PCA into microwave CAD software, it is possible to analyse arbitrary planar structure and obtain its characteristics in terms of the scattering parameters.

1.2 Planar Circuit Models

As the microwave technology in the present times evolves towards the use of higher frequencies and more sophisticated millimeter-wave integrated circuits and components, a considerable theoretical effort is required in order to improve the characterisation and modeling of microwave structures. Hence, a necessity for reliable computer-aided design techniques is felt. In the formulation of CAD techniques, one has to compromise between accuracy and simplicity. The starting point for the development

of CAD programs is characterisation of the structures involved in the circuits. Most of the CAD programs are based on the curve-fitting formulas and look-up tables, exact analysis are often impractical because of exceedingly high computer time required.

From the viewpoint of CAD techniques the planar-circuit approach is a very powerful technique. PCA although basically developed for the analysis of microstrip circuits can be extended to other microwave circuit configurations like reduced height waveguide, stripline, suspended microstrip etc. Though the planar circuit is an approximate model of microstrip components, it constitutes a substantial improvement over conventional transmission-line models, providing accurate descriptions of their performances. On the other hand, planar-circuit models are simple enough to keep the computer analysis reasonably fast and inexpensive.

1.3 Organization of Thesis

This thesis explores the possibility of building a graphical user interface (GUI) based computer program for microwave circuit design, which can be installed on any present day windows based computer system. This graphical user interface can be used by the students of electromagnetic and microwave theory to understand the various complexities of design and analysis of microwave circuit based on the various electromagnetic computational techniques available. The work presented in the thesis is application of the planar circuit approach for the analysis of some basic types of microwave planar structure.

Chapter 2 starts with a survey of some important literatures, on planar circuit approach theory and its applications. It has been used in the design and analysis of a variety of microwave and millimeter wave components. Further, the concept of planar circuit approach to microwave circuit analysis is explained, and the types of microwave circuit elements, which can be modeled as planar circuits are explained. The 2-dimensional circuit theory developed for planar component based on the concept of voltages and currents is discussed. Green's function method as the analysis method has been studied in details with the various boundary conditions taken into consideration. Techniques like Segmentation and Desegmentation, for the analysis of complicated planar configurations are also discussed Concluding chapter provides some insight into the capabilities and limitations of the approach.

In chapter 3, a brief account of discontinuities found in the design of microwave circuits with particular reference to planar circuits, like the microstrip are discussed.

The traditional analysis methods for discontinuities, viz. Quasi-static and Full-wave analysis methods are explained in brief. Finally the applicability of the planar circuit approach for the characterization of discontinuities is indicated.

Chapter 4 deals with the description of the software developed. Next section illustrates the formulation of impedance matrix elements of some typical planar segments with open boundaries Further a couple of examples, viz. rectangular patch, single step and double step are considered to illustrate the applicability of GUI developed based on the Planar circuit approach. Chapter 5 presents the summary, the conclusions and the scope for further work

CHAPTER 2

PLANAR CIRCUIT ANALYSIS

2.1 Introduction

In the past until 1970s, microwave engineers and researchers had generally focused on the three principal categories of electric circuits. These are lumped elements (zero-dimensional) with physical dimensions much smaller than the wavelength, circuits whose dimensions are much smaller in two directions but comparable to the wavelength in the third direction, (one-dimensional) which are transmission line type of distributed elements, and the third category consists of the waveguide type (three-dimensional) of circuits whose all the three directions are comparable to the wavelength. Complimentary to the above stated three categories is a forth category which can be treated as a two-dimensional circuit. This is defined as an electrical circuit having dimensions comparable to the wavelength in two directions, but much less in the third direction [1,2]. Thus the concept of two-dimensional planar circuit was first introduced by Takanori Okoshi, in early 1970s, as an approach for analyzing two-dimensional microwave integrated circuitry (MIC).

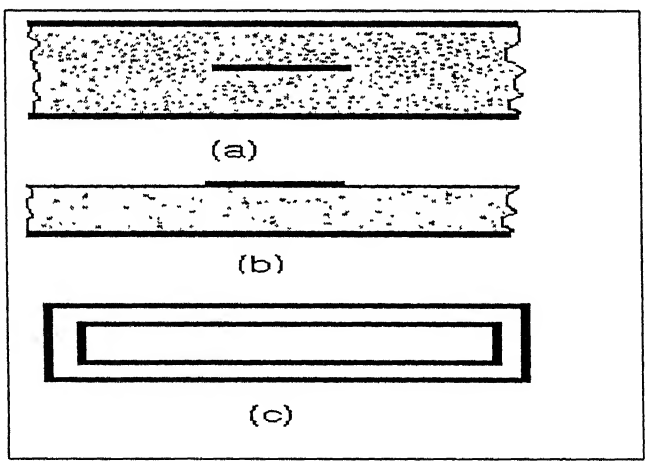

Figure 2.1 Types of planar circuit [1] (a) Triplate type (b) Open Type (c) Cavity Type

In general three types of the planar circuits are possible. They are the triplate type (stripline and stripline-like), the open type (microstrip) and the cavity type (waveguide), as shown in the figure 2 1(a), (b) and (c) respectively. In section 2.2 the main features of planar circuit analysis are summarized, starting from the wave equation and the associated boundary conditions, various methods of excitation, and different methods of solving the wave equation are discussed. In section 2.3, the Green's function approach, which has been used in the thesis for analysis of the planar circuit, is described in detail. In section 2.4, an analysis of planar circuit of composite configuration is considered In section 2.5 capabilities and limitation of the approach are stated.

2.2 Planar Circuit Analysis

2.2.1 The Wave Equation for Planar Structure

Consider a stripline geometry with top and bottom ground planes with an arbitrary patch conductor in the center as shown in figure 2 2. To qualify as a planar circuit the ground plane spacing, 2d, must be very small compared to wavelength of the exciting EM wave, typically $2d<0.1\lambda$. Under the assumption that the **E** field of the structure is mainly along the z-direction, or we can say E field has only E_z component, with $E_x = E_y = 0$. This also implies that the propagation constant, β_z, along the z-axis (see figure 2 2 for the co-ordinate system) is zero, making $k_o^2 \varepsilon_r = \beta_x^2 + \beta_y^2$, where β_x and β_y are the propagation constants along x and y-axis, respectively, k_o is the free space propagation constant and ε_r is the relative dielectric constant of the medium filling the space between the two ground planes.

To analyze this structure using the planar circuit approach, first the periphery of the patch is cut into N pieces of width w_i, $i = 1,2,3 \ldots N$, and each piece of the periphery is treated as a port Thus, the patch conductor of the arbitrary shape is converted to an N-port network. Appropriate terminations such as , open , short or an impedance can be specified for each port depending on the boundary conditions The excitation can be by connecting a source to one of these ports (edge fed microstrip) or one can also excite using coaxial probe connected to the patch at any point via the ground plane (center conductor of the coaxial is connected to the patch at appropriate point and the outer conductor is connected to the ground plane).

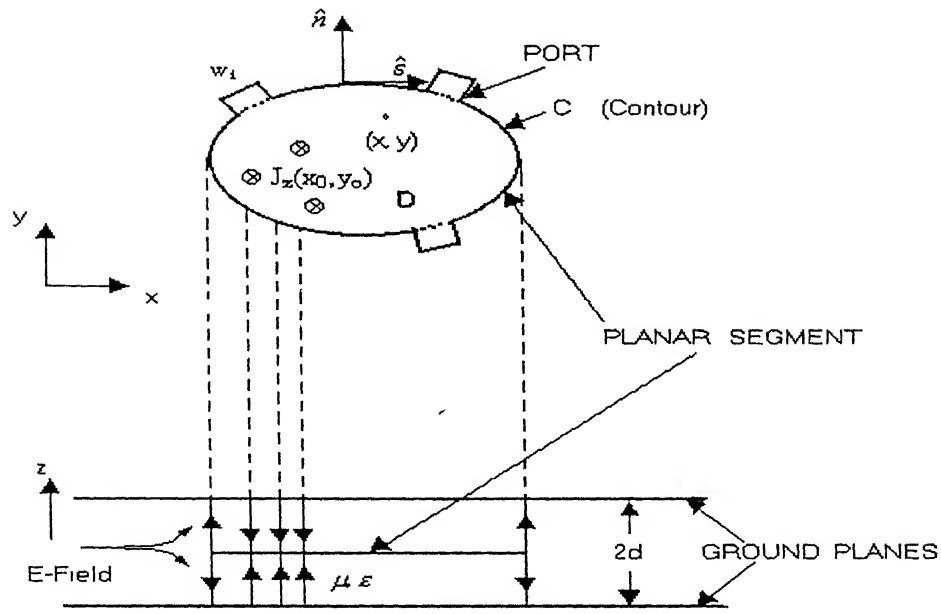

Figure 2.2 Configuration for a typical segment in planar microwave circuits

The coordinates are assumed such that the planar element lies in the xy plane and it is perpendicular to the z-axis. Thus, the dimensions along the x and y coordinate are comparable to the wavelength and the thickness along the z direction is much smaller than the wavelength of the signal. Therefore, the fields inside the circuit can be assumed to be uniform along the z-direction and we can set $\partial / \partial z = 0$ and $H_z = E_x = E_y = 0$. For a homogeneous and isotropic dielectric material, the wave equation (Helmholtz equation) governing the electromagnetic fields of this source-free structure reduces to

$$(\nabla_t^2 + k^2) E_z = 0. \qquad (2\ 1)$$

Where

$$\nabla_t^2 = \partial^2/\partial x^2 + \partial^2/\partial y^2 \qquad (2.2)$$

and

$$k = \omega \sqrt{(\mu \varepsilon)} \qquad (2.3)$$

ω = Angular frequency.

ε = Permittivity of the dielectric (spacing material).

μ = Permeability of the dielectric.

k = Wave number of the dielectric.

2.2.2 Boundary Conditions

The characteristics of the planar circuit are determined by the solution of the 2-dimensional Helmholtz equation (2.1) and the given boundary conditions. The boundary conditions for a given planar circuit are determined by the behavior of the surface current at the periphery. The surface current on a conducting sheet is obtained from the boundary condition

$$\mathbf{J}_s = \hat{n} \times (\mathbf{H}_1 - \mathbf{H}_2), \tag{2.4}$$

where $\hat{n}$ is a unit vector normal to the sheet and $\mathbf{H}_1$ and $\mathbf{H}_2$ are the magnetic fields on the two sides of the conducting sheet. For the central conductor of a stripline type planar circuit, $\mathbf{H}_1 = -\mathbf{H}_2$, and thus

$$\mathbf{J}_s = -2\hat{n} \times \mathbf{H}_2 \text{ (A/m)}. \tag{2.5}$$

Using Maxwell's equations the magnetic field can now be written as

$$\mathbf{H} = -\frac{1}{j\omega\mu} \nabla \times \mathbf{E}, \tag{2.6}$$

which upon using

$$\mathbf{E} = \hat{a}_z E_z(x, y) \tag{2.7}$$

reduces to

$$\mathbf{H} = \frac{1}{j\omega\mu}\left(-\frac{\partial E_z}{\partial y}\hat{a}_x + \frac{\partial E_z}{\partial x}\hat{a}_y\right). \tag{2.8}$$

Where $\hat{a}_x$, $\hat{a}_y$ and $\hat{a}_z$ are the unit vectors along the x, y and z directions respectively. Substituting (2.8) into (2.5) gives

$$\mathbf{J}_s = \frac{2}{j\omega\mu}\left(-\frac{\partial E_z}{\partial y}\hat{a}_x + \frac{\partial E_z}{\partial x}\hat{a}_y\right) \quad \text{(A/m)}. \tag{2.9}$$

The expression of $\mathbf{J}_s$ is valid at all the points on the central conductor (patch), as shown in figure 2.2, including the periphery. But in the case of microstrip type of planar circuit the periphery of the conductor has to be extended to account for the fringing fields, as the upper ground plane of figure 2.2 is not there. Hence, there is no magnetic field above the patch and the factor 2 in (2.5), (2.9) and (2.10) is absent.

For the points on the periphery C, **Js** can be written in terms of components normal and tangential to the periphery C as

$$\mathbf{J_s} = \frac{2}{j\omega\mu}\left(-\frac{\partial E_z}{\partial s}\hat{s} + \frac{\partial E_z}{\partial n}\hat{n}\right) \text{(A/m)}, \qquad (2.10)$$

where $\hat{s}$ and $\hat{n}$ are the unit vectors tangential and normal to the periphery, respectively, as shown in figure 2 2.

The boundary conditions can be given as either open (infinite impedance), shorted (zero wall impedance), or terminated by an impedance wall of finite value, except for the coupling ports located on the periphery. For an open-boundary periphery the normal component of the surface current must be zero, i.e.,

$$\frac{\partial E_z}{\partial n} = 0. \qquad (2.11)$$

The above condition is also referred to as the *magnetic wall boundary condition.* On the other hand, for a short-circuited part of the periphery of the planar circuit, the tangential component of the electric field must be zero, i e.,

$$E_z = 0 \ . \qquad (2.12)$$

This condition is known as the *electric wall boundary condition.* When the periphery is terminated by an arbitrary impedance, Z_w, then it must satisfy the wall impedance boundary condition given as

$$Z_w = |E_z / H_s|, \qquad (2.13)$$

where the electric field E_z defines a voltage v between the planar circuit conductor and the ground plane. Since E_z is constant along z, this voltage is given as

$$v = - E_z d, \qquad (2.14)$$

where d represents the spacing between the two conductors, patch and the ground plane as shown in the figure 2.2

2.2.3 Methods of Excitation

The excitation of electromagnetic fields inside a planar structure can be done either through some aperture at the lateral wall to couple the planar structure to the

external circuit (edge-fed microstrip/stripline) or by some internal current source J_z (by coaxial lines). In the coaxially fed microstrip type of planar circuit, the coaxial feed is perpendicular to the circuit, with the outer conductor of the coaxial line connected to the ground plane and inner conductor protruding through the substrate and touching the top conductor of the microstrip line type of planar circuit. For the stripline type of planar circuit both the ground planes are to be connected to the outer conductor of the coaxial feed and inner conductor (planar circuit) to be connected to the inner conductor of coaxial feed. The excitation current $i_z(x_o, y_o)$ is be the same as the current flowing in the center conductor of the coaxial line.

On the other hand, for the edge-fed planar circuit the strip conductor of the feeding line is connected to the periphery of the conducting patch. The excitation current now flows (at the coupling port) normal to the periphery of the planar circuit. This current can be obtained from (2.10) by integrating the normal component of the current density over the coupling port width W, and is given by

$$i = -\frac{p}{j\omega\mu}\int_w \frac{\partial E_z}{\partial n} ds, \tag{2.15}$$

where $p = 1$ for microstrip-type planar circuit and $p = 2$ for stripline-type planar circuit, and ds is the incremental distance along the periphery. The negative sign in (2.15) implies that the current i flows inwards, whereas $\hat{n}$ in (2.10) points outwards. The planar components with open boundary can now be characterized in terms of the voltage v on the conducting patch. Substituting (2.14) in (2.1), (2.11) and (2 15) we get

$$(\nabla_t^2 + k^2) v = 0, \tag{2.16}$$

along with

$$\frac{\partial v}{\partial n} = 0, \tag{2.17}$$

for points on the periphery where there are no coupling ports. The current flowing into the coupling port is expressed as

$$i = \frac{p}{j\omega\mu d}\int_w \frac{\partial v}{\partial n} ds. \tag{2.18}$$

The solution of the wave equation (2.16), along with (2.17) and (2.18) as the boundary conditions, has been evaluated in the thesis for characterization of the planar circuit. In the next section a brief overview about the various analysis techniques available for the solution of the 2-dimensional wave equation is given.

2.2.4 Analysis Techniques

The solution for the wave equation along with the boundary conditions governing planar circuits with isotropic media can be obtained by various analytical and numerical techniques. The choice of any technique primarily depends on the geometry of the conducting patch (planar circuit) and also the desire to have compact analytical expression and /or to have more efficient computer use [6].

For the planar circuits of simple geometrical shapes (rectangle, triangle etc) the Green's function approach and the eigen-mode expansion approach are the most convenient. When the geometrical shape of the planar circuit is neither simple nor completely arbitrary, but it is a composite of simple shapes for which the Green's functions are available in the literature, the segmentation method can be used [3,4]. Using the segmentation method, the characteristics of overall circuit can be obtained from those of the simpler segments. Another complementary analysis technique desegmentation [9,10] can be used, where some simple shapes can be added to the given planar circuit to result in another simple shape. In this case the characterisation of the given planar circuit is obtained from the shapes added and the resultant shape. The technique of Green's function approach with the segmentation and desegmentation has been used in this thesis for the characterisation of planar circuits with the help of some examples. Green's function approach is explained in details in the next section

If the geometrical shape of the planar circuit is completely arbitrary and neither the segmentation nor the desegmentation approach can be applied, numerical methods such as finite element approach (extension of finite elements method) and /or the contour integral method (boundary integral method) are used to characterize a planar circuit [6].

2.3 Green's Function Approach

The Green's function, which gives the voltage at any point on the planar circuit for a unit current source excitation, is the basis of this approach. The Green's function for a particular geometrical shape is to be obtained analytically. When the location of

the ports is specified, the impedance matrix characterizing the planar components can then be easily derived using the Green's function.

Let the planar component be excited by a current density $\mathbf{J}_z$ in the z direction at any arbitrary point (x_o, y_o) inside the periphery as shown in the figure 2.2, the wave equation can now be written as

$$(\nabla_t^2 + k^2)\, v = -j\omega\mu\, d\mathbf{J}_z\,, \tag{2.19}$$

where ∇_t and k are as defined in (2 2) and (2.3) ,respectively. If the planar circuit is edge-fed or exited by a stripline, a fictitious current density, $\mathbf{J}_z$, is injected normally into the circuit. In this case the current density injected into the circuit at coupling ports located along the periphery can be equivalently considered as fed normal to the circuit, along the z direction, with the magnetic wall condition $\partial v/\partial n = 0$ being imposed all along the periphery. The equivalent fictitious surface current, $\mathbf{J}_s$ (in the z direction) obtained from the boundary condition (2 4) may be written as

$$\mathbf{J}_s = \frac{1}{j\omega\mu d}\frac{\partial v}{\partial n}\hat{a}_z \text{ (A/m)}. \tag{2.20}$$

Hence, it is seen that for both the methods of excitation, the planar circuit can be considered as being excited by z-directed line currents located at the coupling ports. Also magnetic wall boundary condition is imposed all along the periphery of the planar circuit.

The Green's function $G(\mathbf{r}/\mathbf{r}_o)$ for eqn (2.19) is obtained by applying a unit line current source $\delta\ (\mathbf{r} - \mathbf{r}_o)$ flowing along the z-direction in the region below the central patch and located at $\mathbf{r} = \mathbf{r}_o$. The Green's function $G(\mathbf{r}/\mathbf{r}_o)$ is a solution of

$$(\nabla_t^2 + k^2)\, G(\mathbf{r}/\mathbf{r}_o) = -j\omega\mu\, d\delta\,(\mathbf{r} - \mathbf{r}_o). \tag{2.21}$$

With the boundary condition at the periphery given by

$$\frac{\partial G}{\partial n} = 0. \tag{2.22}$$

The voltage at any point on the planar circuit can be written as

$$v(x,y) = \iint_D G(x,y/x_o,y_o) J_z(x_o,y_o)\, dx_o dy_o, \qquad (2\ 23)$$

where $J_z(x_o, y_o)$ is the fictitious source current normally injected into the circuit and D is the two-dimensional region of the planar circuit enclosed by the magnetic walls. For a case where the source current is injected only at the periphery (edge-fed), the voltage v at the periphery can be written as

$$v(s) = \int_c G(s/s_o) J_s(s_o)\, ds_o, \qquad (2.24)$$

where $J_s(s_o)$ is the z-directed current source given by (2.20), s and s_o are the distances measured along the periphery, and the integral along the right hand side is over the entire periphery C. Further, as the line current $J_s(s_o)$ is present only at the coupling ports, that represent a discrete number of sections on the periphery, (2.24) may be written as

$$v(s) = \sum_j \int_{W_j} G(s/s_o) J_s(s_o)\, ds_o, \qquad (2.25)$$

where W_j indicates the width of the jth coupling port, and the summation is over all the coupling ports. Also from (2 18) and (2.20) the current i_j fed at the jth port can be written in terms of the z-directed equivalent line current as

$$i_j = p \int_{W_j} J_s(s_o) ds_o. \qquad (2.26)$$

The widths of the coupling ports are assumed to be small so that the line current density, J_s, is distributed uniformly over the width of the port. Hence from (2.26) we have

$$J_s(s_o)\,|_{for\ jth\ port} = \frac{i_j}{pW_j}. \qquad (2.27)$$

Substituting (2.27) into (2.25), the expression for the voltage at any point on the periphery, v(s), can be written as

$$v(s) = \sum_j \frac{I_j}{pW_j} \int_{W_j} G(s/s_o) ds_o \,. \tag{2.28}$$

To find the voltage v_i at the i^{th} port, the average of $v(s)$ over the width of the port is taken as follows

$$v_i = \frac{1}{W_i} \int_{W_i} v(s) ds. \tag{2.29}$$

The expression for v_i is found by substituting (2 28) in (2.29) as

$$v_i = \sum_j \frac{I_j}{pW_iW_j} \int_{W_i} \int_{W_j} G(s/s_o) ds_o ds \,. \tag{2.30}$$

By dividing both sides of (2.30) by i_j, the elements of the impedance matrix of the planar circuit can be written as

$$z_{ij} = \frac{1}{pW_iW_j} \int_{W_i} \int_{W_j} G(s/s_o) ds_o ds, \tag{2.31}$$

where $p = 1$ for microstrip-type planar circuit and $p = 2$ for stripline-type planar circuit. Using (2.31) the impedance matrix Z of the planar element can be constructed, and then the scattering matrix can be determined using the relation

$$S = \sqrt{Y_o}\,(Z - Z_o)(Z + Z_o)^{-1} \sqrt{Z_o}\,, \tag{2.32}$$

where Z_o, $\sqrt{Z_o}$ *and* $\sqrt{Y_o}$ are the diagonal matrices with diagonal elements given by

$Z_{01}, Z_{02}, \ldots, Z_{0n}$, $\sqrt{Z_{01}}, \sqrt{Z_{02}}, \ldots\ldots, \sqrt{Z_{0n}}$; and $1/\sqrt{Z_{01}}, 1/\sqrt{Z_{02}}, \ldots\ldots, 1/\sqrt{Z_{0n}}$; respectively. The matrix elements $Z_{01}, Z_{02}, \ldots, Z_{0n}$, represent the normalizing impedances at the various ports of the planar circuit.

In the above analysis, the widths W_i of the coupling ports are assumed to be small in comparison to the wavelength and the dimensions of the planar component, so that the injected current in each port is distributed uniformly over the width of the port. For cases where the above assumption is not valid, each coupling port is divided into a number of subports over which the injected current can be assumed to be uniformly distributed .The impedance matrix is now constructed with all the subports included Now the multiple subports are combined into a single port based on the observation that the voltages at the two connected subports are equal even though the currents may be different.

Since the voltages at the subports are equal, the subports can be considered to be connected in parallel. The combination of subports requires inversion of the Z matrix to obtain the admittance matrix, Y. In general, if ports i and j are divided into n and m subports, respectively, such that $i = \{i_1, i_2, ..., i_n\}$ and $j = \{j_1, j_2, ..., j_n\}$, then the term Y_{ij} of the overall admittance matrix is given as

$$Y_{ij} = \sum_{k=1}^{n} \sum_{l=1}^{m} Y_{kl} , \qquad (2.33)$$

where Y_{kl} are the elements of the admittance matrix with multiple subports. The overall scattering matrix can now be obtain from the impedance matrix using (2.32) or directly from the admittance matrix using

$$S = \sqrt{Z_o}\,(Y_o - Y)(Y_o + Y)^{-1}\sqrt{Y_o} , \qquad (2.34)$$

where Y_0 is a diagonal matrix of normalizing admittances at various ports with diagonal elements given by $1/Z_{01}, 1/Z_{02}, ..., 1/Z_{0n}$.

2.4 Analysis of Planar Circuit of Composite Configuration

The impedance matrix for a planar circuit with a regular geometrical shape can be obtained from the Green's function when port locations are specified. On the other hand, segments with completely arbitrary shapes, for which a Green's function cannot be written, necessitate the use of the contour integral method to compute the impedance matrix. Between these two extreme cases, there is a class of planar components in which the shape of the planar circuits is a composite simple configuration. In these cases, the two-dimensional composite shapes can be decomposed into either

(a) All regular shapes ,or

(b) A combination of some regular shape(s) and some arbitrary shape(s)

This process of breaking down a composite shape into simpler shapes is known as *segmentation* [3,4,5].

There is also a complementary process called *desegmentation*, which is suitable for analyzing some planar circuit configurations. It has been shown that if the impedance matrices the segments added to the original configuration and the impedance matrix of the augmented configuration are known, the impedance matrix of the original planar

segment can be obtained by using desegmentation formulas [9,10].

2.4.1 Segmentation Method

The basic formulation of this method is to divide a single complicated planar circuit configuration into simpler *segments* that have regular shapes and can therefore be characterized relatively easily. An example of such a segmentation is shown in figure 2.3, where a microstrip patch is broken down into two rectangular segments for which Green's function is available. Essentially, the segmentation method gives us overall characterization or performance of the composite network when the characterization of each of the segments is known. Originally the segmentation method was formulated [3,4] in terms of S matrices of individual segments however, it was found subsequently [5] that a Z matrix formulation is more efficient for microwave planar circuits. In the thesis the segmentation procedure used based on Z matrices.

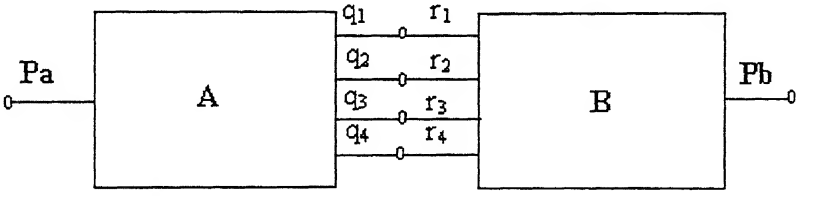

Figure 2.3 Ports nomenclature used in the segmentation formula

This procedure of segmentation is illustrated by considering a multiport network consisting of only two segments A and B as shown in figure 2.3. The various ports of these two segments are numbered. The external (unconnected) ports of segment A are called Pa ports, and the external unconnected ports of segment B are referred to as Pb ports. The connected ports of segment A are called q ports, and the connected ports of segment B are designated r ports. The q and r ports are numbered such that q_1 is connected to r_1, q_2 to r_2, and so on. As a result, of these interconnections the voltages and currents will be

$$v_q = v_r \qquad \text{and} \qquad i_q = -i_r . \tag{2.35}$$

The Z matrices of segments A and B may be written as

$$Z_A = \begin{bmatrix} Z_{Pa} & Z_{Paq} \\ Z_{qPa} & Z_{qq} \end{bmatrix} \quad \text{and} \quad Z_B = \begin{bmatrix} Z_{Pb} & Z_{Pbr} \\ Z_{rPb} & Z_{rr} \end{bmatrix}, \qquad (2.36)$$

where Z_{Pa}, Z_{Paq}, Z_{qPa}, Z_{qq}, Z_{Pb}, Z_{Pbr}, Z_{rPb}, Z_{rr} are submatrices of appropriate dimensions depending on no of ports. Since these components are reciprocal, the following relationships apply:-

$$Z_{Paq} = [Z_{qPa}]^t \quad \text{and} \quad Z_{Pbr} = [Z_{rPb}]^t, \qquad (2.37)$$

where the superscript t denotes the transpose of the matrix.

The Z matrices of the segments A and B are written together as

$$\begin{bmatrix} V_P \\ V_q \\ V_r \end{bmatrix} = \begin{bmatrix} Z_{PP} & Z_{Pq} & Z_{Pr} \\ Z_{qP} & Z_{qq} & 0 \\ Z_{rP} & 0 & Z_{rr} \end{bmatrix} \begin{bmatrix} i_P \\ i_q \\ i_r \end{bmatrix}, \qquad (2.38)$$

where

$$v_p = \begin{bmatrix} v_{Pa} \\ v_{Pb} \end{bmatrix} \quad and \quad i_p = \begin{bmatrix} i_{Pa} \\ i_{Pb} \end{bmatrix},$$

and

$$Z_{PP} = \begin{bmatrix} Z_{Pa} & 0 \\ 0 & Z_{Pb} \end{bmatrix} \quad Z_{Pq} = \begin{bmatrix} Z_{Paq} \\ 0 \end{bmatrix} \quad Z_{Pr} = \begin{bmatrix} 0 \\ Z_{Pbr} \end{bmatrix} \quad Z_{Pq} = [Z_{qP}]^t \quad Z_{rP} = [Z_{Pr}]^t$$

,where 0 denotes a null matrix of appropriate dimensions. The relation given by (2.37) is substituted in (2.38) to eliminate v_q, v_r, i_q and i_r. The resulting expression can be written as $v_P = [Z_{AB}]\, i_P$, where

$$[Z_{AB}] = \begin{bmatrix} Z_{Pa} & 0 \\ 0 & Z_{Pb} \end{bmatrix} + \begin{bmatrix} Z_{Paq} \\ -Z_{Pbr} \end{bmatrix} [Z_{qq} + Z_{rr}]^{-1} [-Z_{qPa} + Z_{rPb}]. \qquad (2.39)$$

In the above equation the size of Z_{AB} is (Pa + Pb) × (Pa + Pb) .The second term on the right-hand side of equation is a product of three matrices of sizes (Pa + Pb) × q, q × q and q × (Pa + Pb) .From the computational point of view , the most time–consuming step is the evaluation of the inverse of the matrix $[Z_{qq} + Z_{rr}]$.

2.4.2 Desegmentation method

There are several configurations of planar circuits that cannot be analyzed by the segmentation method discussed above Some configuration, that cannot be partitioned into regular segments for which Green's functions are known but can be combined with other regular shapes to give an overall regular shape. For such cases, an alternative method called desegmentation [9, 10] is used. The process of desegmentation can be illustrated by considering the example shown in figure 2.4. If a circular sector called segment β is added to the configuration α, the resulting configuration γ is a triangular segment. Green's functions are known for both circular sector and triangular shapes, and therefore Z matrices for characterizing both of these components may be derived.

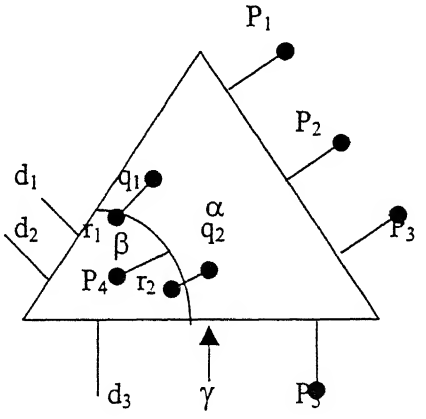

Figure 2.4 Ports nomenclature used in the desegmentation formula

The desegmentation method allows us to derive the Z matrices of the original configuration α when the Z matrices of the triangular segment γ and the circular sector segment β are known. The relationship among the Z matrices of three shapes are derived by considering various external and connected ports located as shown in Figure 2.4. Ports P_1, P_2,..., are external ports of α. Characterization of α is required with respect to these ports. In general, p ports can also be located on the part of the periphery of α where the segment β is connected. An example of this is the port P_4 shown in the figure. The Z matrices of β and γ segments are known and can be written as

$$Z_\beta = \begin{bmatrix} Z_{rr} & Z_{rd} \\ Z_{dr} & Z_{dd\beta} \end{bmatrix} \qquad Z_\gamma = \begin{bmatrix} Z_{PP\gamma} & Z_{Pd} \\ Z_{dP} & Z_{dd\gamma} \end{bmatrix} \tag{2.40}$$

As in the case of segmentation, ports q (of α) and ports r (of β) are numbered such that q_1 is connected to r_1, q_2 to r_2 etc Ports d are the unconnected (external) port of the segment β. Evaluation of Z_α is simplified when the number of d ports is made equal to the number of q (or r) ports. The numbers of q (or r) ports depends on the nature of the field variation along the α-β interface and, as in the case of segmentation, is determined by iterative computations. On the other hand, the number of d ports is arbitrary and can be made equal to that of q (or r) ports after the number of q ports has been finalized. Under these conditions, the impedance matrix for the α segment can be expressed [9] in terms of the Z matrices of the β and γ segmentation as

$$Z_\alpha = Z_{PP\gamma} - Z_{Pd}\{Z_{dd\gamma} - Z_{dd\beta}\}^{-1} Z_{dP} \tag{2.41}$$

It may be noted that the size of Z_α is P × P since all the specified ports of α segment have been numbered as p ports.

2.5 Capabilities and Limitations

The advantages of the planar circuit approach are as follow [6]: -

(a) The planar circuit has wider freedom in the circuit design than the stripline or microstrip circuit does. One- dimensional stripline and microstrip circuit may be treated as special case of 2-dimensional circuits. The planar circuit can offer a lower impedance level than the stripline circuit does. In MIC actual line lengths become small at high frequencies and line widths become large for low impedance levels (which are normally needed for use with MIC). In such cases, PCA yields better characterizations of MICs than offered by transmission line approach [15].

(b) PCA is also applicable to the analysis of discontinuities in stripline and microstrip lines. By optimizing the discontinuity configuration, its effect can be compensated to improve performance of the circuit [17].

(c) Several new designs can be obtained by using PCA. For example it has been shown [19] that a circular disc resonator can also be used as a 3-db hybrid

(d) Planar circuits, fabricated on the ferrite substrates, and may also be analyzed by PCA by extension of techniques used for analyzing circuits on dielectric substrates.

(e) In microstrip antennas, the aperture field distribution can also be evaluated by treating them as planar components with magnetic walls. PCA can be used to evaluate the field along the periphery of these components.

(f) With the use of photoetching techniques, planar circuits are easier to fabricate than the three-dimensional waveguide circuits.

The limitations of the planar circuit approach are as follows: -

(a) The PCA can be used only for the design of passive MIC components

(b) The microstrip components are approximate planar circuits, as the electromagnetic fields are not entirely confined to the substrate region. Suitable modification in terms of effective parameters is made to account for the stray fields.

(c) The PCA does not provide full wave three-dimensional analysis of microwave circuits.

CHAPTER 3

DISCONTINUITIES AND MODAL ANALYSIS

3.1 Introduction

This chapter deals with the discontinuities found in the microwave circuits, their analysis and applicability of planar circuit theory to characterize them. The basic building blocks of the microwave integrated circuits are the sections of uniform transmission structures viz. waveguide, stripline, microstrip line, coplanar waveguide coplanar strips, slot line coupled striplines etc. Microwave integrated circuits invariably involves discontinuities of one type or another in the strip conductor. These discontinuities result from abrupt changes in the geometry of the strip conductors. In some cases these discontinuities are unavoidable, and are results of mechanical or electrical transitions. The effect of discontinuities on the circuit performance is significant at microwave frequencies, and hence must be characterized and accounted for in the design of the circuits. In some cases discontinuities may be deliberately introduced into the circuit to perform a certain electrical function.

A transmission line discontinuity can be represented as an equivalent circuit at some point on the transmission line. Depending on the type of discontinuity, the equivalent circuit can be a simple shunt or series element across the line or as a general case it will be a T-or-π equivalent circuit. The component values of an equivalent circuit depend on the parameters of the line and the discontinuity, as well as the frequency of operation. In some cases the equivalent circuit will involve shift in the reference planes on the transmission lines. After the equivalent circuit of a given discontinuity is formulated its effects are incorporated in the analysis or design of the MIC.

3.2 Discontinuities Encountered in Planar Circuits

Discontinuities are associated with all types of transmission line structures. Coaxial line and waveguide discontinuities have extensively been treated in the literature An accurate characterisation of discontinuities is considered essential for MIC. This is because of the fact that the microstrip circuits can not be adjusted or tuned after the circuit

is fabricated. If a provision for adjustments, is made then the main advantages of compactness and reproducibility gained by use of MIC technology is lost to some extent. Therefore, the microstrip and stripline discontinuities have been studied extensively and characterized. Some typical types of the discontinuities encountered in the microwave planar circuits, can be outlined as follows [11]: -

(a) Abruptly ended strip conductor (open circuit).

(b) Rectangular conductor patch.

(c) Step change in width (introduced form change in impedance level).

(d) Slot in the strip conductor.

(e) Right angled bend.

(f) Tee junctions.

The reactances associated with these discontinuities are also called parasitic in literature, as they are not introduced intentionally. In general, the dimensions of the discontinuities are much smaller than the wavelength. Hence, equivalent circuits consisting of various lumped elements can approximate these discontinuities. The discontinuities listed above and their equivalent circuits are shown in figure 3.1. The analysis procedure available in the literature is given briefly in the following section.

3.3 Analysis Procedure

For most of the uniform transmission structures used in microwave circuits, the fields are completely described by a single propagating mode. In contrast, the complete description of the fields at the discontinuity region generally requires an infinite number of non-propagating modes in addition to the propagating mode. However the non-propagating modes or the higher order modes restrict their field distribution to the immediate vicinity of the discontinuity. Hence, the discontinuity fields can be effectively regarded as localised. The complete characterisation of a discontinuity involves determination of frequency dependent scattering matrix coefficients associated with the discontinuity. These types of analysis are available for the above stated types of discontinuities for microstrip line and stripline structures in literature. Discontinuities in MIC involve an abrupt change in the dimensions of the strip conductor, giving rise to perturbations in the electric and the magnetic field distributions. The stored energy in the changed electric field distribution can be represented by an equivalent capacitance, and the stored energy in the changed magnetic field distribution can be expressed in terms of an equivalent inductance. In both cases only the evanescent mode energy contributes to

the stored energy. The discontinuity is characterized by evaluating these capacitances and inductances.

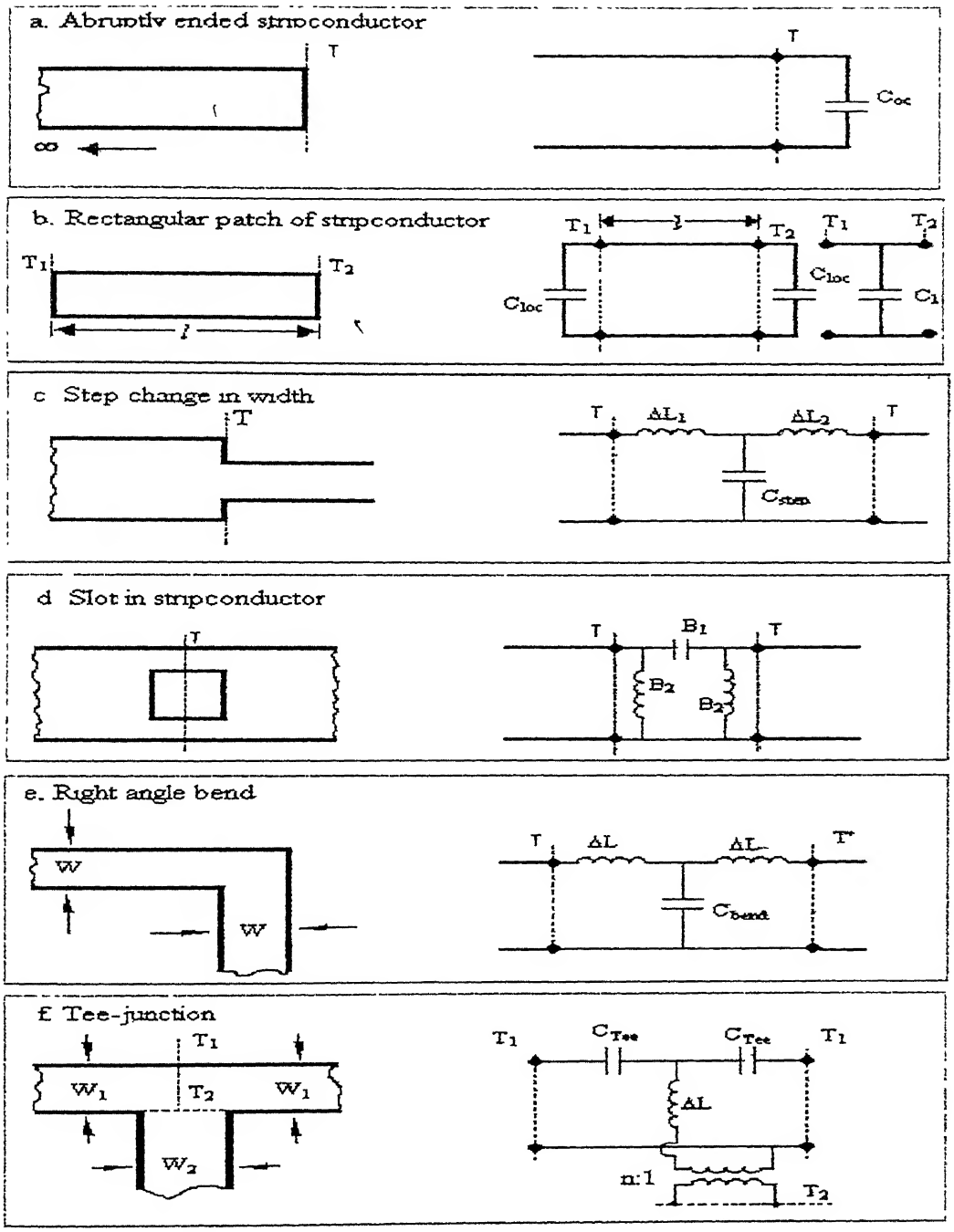

Figure 3.1 Various types of microwave discontinuities and their equivalent circuit [8].

Analysis of these discontinuities can either be based on the quasi-static considerations or carried out more rigorously by full-wave analysis. Quasi–static analysis involves calculations of static capacitances and low frequency inductances. Equivalent circuits for discontinuities can be derived form these results. Alternatively, a waveguide type dynamic analysis taking dispersion and higher order modes also into account can be carried out. This will lead to a frequency depended scattering matrix. Here also, equivalent circuits for discontinuities are based on these results.

3.3.1 Quasi-Static Approach

The static values of capacitances associated with discontinuities can be evaluated by finding the excess charge distribution near the discontinuity. There are number of quasi-static methods available for calculations of capacitances as given below:-

(a) Matrix inversion method
(b) Variational method
(c) Galerkin's method in the spectral domain, and
(d) Use of line sources with charge reversal

In all of the above methods the following assumptions are implied:-

(a) The size of the discontinuity is small compared to the wavelength so that the phase variation across the discontinuity can be neglected.
(b) The current on the strip has zero divergence.
(c) The strip conductor is infinitely thin.

In several types of discontinuities e.g. bends, steps, T-junctions etc., inductive effects also become significant These inductive components are frequency dependent, and quasi-static calculations provide only their low frequency values. For the calculation of inductances the presence of dielectric substrate (if non-magnetic) is disregarded and only the discontinuity structure and its image in the ground plane are considered. But for magnetic substrate the multiple images formed are also considered.

3.3.2 Full-wave Analysis

Quasi-Static characterisation of capacitances and inductances associated with discontinuities give results that are valid, with sufficient accuracy, only up to a few gigahertz. For the complete characterisation of discontinuities, the frequency dependence of various parameters is required to be found out. This information is obtained from full-wave analysis. Full-wave analysis can be carried out by the following methods: -

(a) Galerkin's method in Finite Time Domain(FTD).

(b) Planar waveguide model.

3.3.3 Characterisation of Various Discontinuities

Based on the results of the above mentioned analysis techniques closed form expression for the capacitances and inductances of various commonly found discontinuities are calculated and are available in literature [6, 11,12] with the ranges for their validity specified. Some of these discontinuities and their equivalent circuits are shown in figure 3.1. Hence, for example, the analysis of discontinuities in stripline, the strip width W of the center conductor is increased by a factor δ, which is depended on the substrate height b and W. The equivalent circuit of an open-ended stripline is represented by an excess capacitance. It can also be represented as equivalent length of a transmission line Δl, which will be depended on circuit parameters like dielectric constant, frequency besides W and b and also Z_0 the characteristic impedance of the stripline.

3.4 Planar Circuit Formulation for Discontinuities

The analysis of microstrip discontinuities using planar circuit approach is based on the waveguide model representation [14,15] of microstrip lines. In the planar waveguide model, the width and the substrate permittivity ε_r of the microstrip line are replaced by an equivalent width $W_e(f)$ and an effective dielectric constant $\varepsilon_{re}(f)$. In the planar waveguide model, two magnetic walls are located along the sides of the equivalent planar waveguide whose width is W_e. The values of W_e and ε_{re} are found by equating the characteristic impedance Z_0 and the phase velocity, v_p, *of* the microstrip line to those of the equivalent waveguide structure. As Z_0 and v_p for the microstrip lines are the functions of frequency, W_e and ε_{re} also become frequency dependent as well, and the dispersion effects due to higher order modes are thus incorporated in the formulation in an approximate manner.

The analysis of discontinuities in the microstrip lines is based on the segmentation and desegmentation methods, already explained in sections 2.4.1 and 2.4.2, applied to equivalent planar waveguide configurations. The applicability of the segmentation and desegmentation methods to the analysis of microstrip line discontinuities is explained by taking an example [17] of a microstrip line right-angled bend discontinuity as shown in figure3 2 (a).

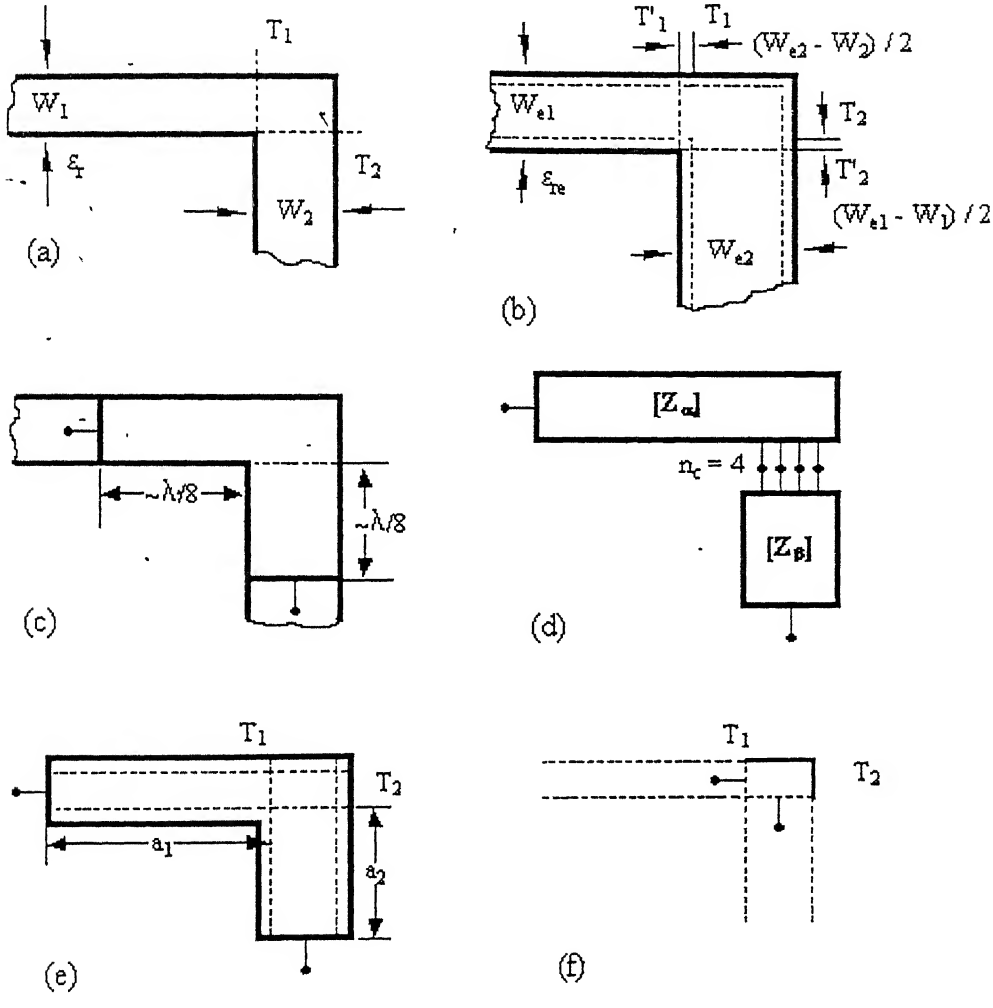

Figure 3.2 An illustration of the segmentation method for analyzing microstrip discontinuity.

The various steps included in this procedure are listed as follows:-

(a) Calculation of the equivalent planar waveguide model of the discontinuity configuration as shown in figure 3.2(b).

(b) Specify the location of the terminal planes (two in the case of the bend) where the external ports are located. These ports are located far away from the discontinuity so that only the dominant microstrip mode is present at the location of the external ports and the higher order evanescent modes have been decayed out, figure 3.2(c).

(c) Decompose the planar configuration into regular segments suitable for analysis by the segmentation or desegmentation method. In the present case segmentation, figure 3.2(d).

(d) Compute the Z matrix for each of the multiport segment using Green's function approach, as explained in section 2.3.

(e) Combine the individual Z matrices into an overall Z matrix for the overall discontinuity configuration.

(f) Convert the Z matrix into a more commonly used S matrix representation.

(g) Transfer the reference planes to the desired locations with respect to the physical configuration of the discontinuity as shown in figure 3.2(e).

From the above procedure it is seen that the planar circuit approach can calculate the required S matrix of the discontinuity without actually restoring to the formulation of an equivalent structure of conductance and inductance. In addition to the characterisation of the discontinuity the planar circuit approach can also be used for the compensation of the microstrip discontinuity reactances. The compensation of the discontinuity reactances involves a modification of the discontinuity's geometrical configuration so as to minimize its adverse effects on the performance of the microstrip circuits.

A combination of the segmentation and desegmentation methods is used for characterisation of the compensated discontinuity. The compensation of the discontinuity can be done by cutting a triangular shape (whose green's function is available) from one or both of the original geometry by using desegmentation method. In the next step segmentation can be used for the characterisation of the compensated discontinuity as explained earlier.

CHAPTER 4

PLANAR COMPONENTS ANALYSIS: EXAMPLES

4.1 Introduction

In this chapter, the applicability of the graphical user interface developed for design and analysis of microwave circuits based on the planar circuit model is explained with the help of examples. Firstly, a brief description of the software developed is provided. The code has been written in MATLAB for both the graphical user interface and also for the computation and analysis of the electromagnetic and microwave circuit parameters. The next section deals with the basic building blocks of the Green's function approach i.e. the Green's function for some geometrical shapes. The Green's function referred to here for 2-dimensional component is the solution of the 2-dimensional wave equation for a unit current source excitation, as discussed in chapter 2. The impedance matrices for planar segments with regular shapes are then analytically evaluated form their respective Green's functions.

Finally to illustrate the utility of the graphical user interface developed, based on planar circuit approach, a couple of examples are taken up. A rectangular patch is analyzed by formulating the S parameters of a two port network. This patch is analyzed both as an individual element and as a combination of two smaller patch using segmentation method, and the results compared. The results for two more type of structure namely a single step discontinuity and a double step discontinuity are also analyzed in terms of S parameters.

4.2 Description of Software

The coding work required for the software, "Integration of the planar circuit analysis into a Microwave Circuit design software", as the name suggests is in two different domains. Firstly, there was a requirement to develop a basic framework of graphical user interface required for microwave circuit design software. Secondly, there

was a requirement to write code using various mathematical tools to solve for the microwave circuit design and analyze the circuit using computational electromagnetic technique, planar circuit analysis The first requirement called for powerful visual programming tools like Visual Basic and the other requirement warranted a language, which gave some flexibility to perform complex calculations and matrix manipulations Initially the possibility for integration of the above mentioned two programs was explored and found that it has not been tried here and it can only be done at the executable program level, which results in non-flexibility at the time of the software development. Hence the decision was taken to use a single program, and the choice was MATLAB. MATLAB being a flexible computing language capable of solving essentially any technical problem also provides a graphical user interface tool.

For the graphical user interface a code was written to load a main figure, something akin to a MATLAB command window, which provides for the basic functions of open, save, printing and editing of files. This main figure is made the working window and menu items where provided for taking the various inputs form the user and providing the results as output. An input data figure is designed to take data about the MIC board, viz. design frequency, permittivity and permeability of the substrate, height of substrate etc. These values are checked for correctness and stored in a file for further use. Another set of inputs is designed to take the data in relation to the planar circuit and provide the S-parameters both numerically and graphically.

Next, the major part of program is the codes written for the planar circuit analysis. This includes the codes for generation of port dimensions, calculation of width and other frequency dependent parameters based on planar waveguide model. Codes for calculation of impedance matrices for rectangular, right-angled isosceles triangle and right-angled 30°-60° triangle based on these widths and combination of parallel port impedance matrix were written. Coding for segmentation and desegmentation procedures, conversion of impedance matrices into S matrices and vice-versa, saving the various results as databases, and finally generating the plots for S–parameters is written. These codes are arranged as different modules that can be called as per the requirement of the main program.

4.3 Green's Functions and the Corresponding Impedance Matrices

The evaluation of Green's functions for a given shape of 2-dimensional component requires solution of the wave equation, having a unit line current source $\delta(\mathbf{r} - \mathbf{r}_o)$ flowing along the z-direction in the region below the central patch and located at $\mathbf{r} = \mathbf{r}_o$, i.e.,

$$(\nabla_t^2 + k^2)\, G(\mathbf{r}/\mathbf{r}_o) = -j\omega\mu\, d\delta(\mathbf{r} - \mathbf{r}_o), \tag{4.1}$$

with the boundary condition at the periphery given by

$$\frac{\partial G}{\partial n} = 0. \tag{4.2}$$

There are two methods available for obtaining Green's functions

(a) The method of images.

(b) The expansion of green's function in terms of eigenfunctions.

The procedure of obtaining Green's function by method of images is follows. An analytical solution of the differential equation (4.1) can be obtained if the right- hand side is a periodic function [20] .For this purpose, additional current sources of the types $\delta(\mathbf{r} - \mathbf{r}_s)$ are placed at the points $\mathbf{r}_s$ outside the region of the planar component. These additional sources can be obtained by taking multiple images of the line source at $\mathbf{r}_o$ with respect to the various magnetic walls or electric walls of the planar component. The source term in (4.1) is modified, and the boundary condition is satisfied by the voltage v produced by the source and its images. It is noted that these additional sources are all outside the region of the planar component and therefore the solution G still represents the green's function for the geometrical shape of the planar component. For a rectangular planar component, the positions of additional line current sources are shown in the figure 4.1. The source pattern used in figure 4.1 is now periodic and therefore its Fourier series expansion can be obtained.

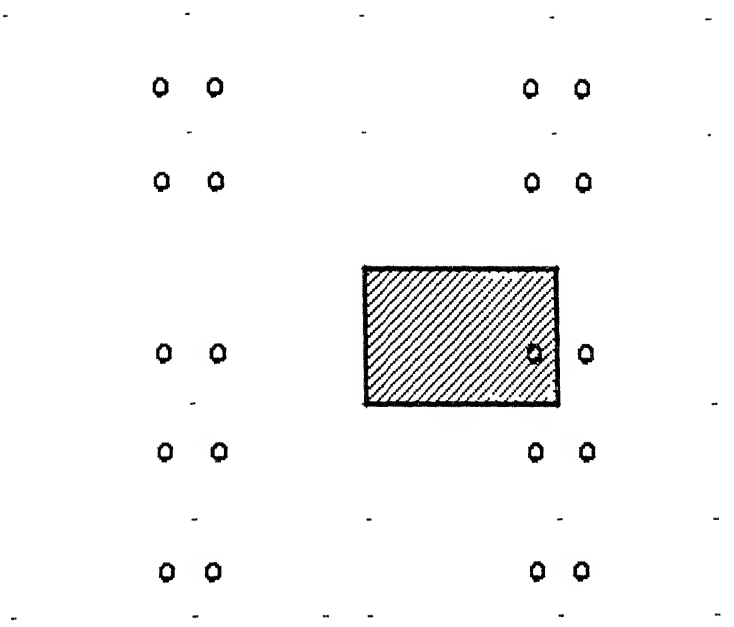

Figure 4.1 Line current source and its images for calculating Green's function of a rectangular component.[6]

The Green's functions can then be expressed as an infinite series summation of the functions obtained as the Fourier series expansion, and these are the eigenfunctions. The coefficients in the series summation for the Green's function can be obtained by substituting the series summation in (4.1).

The method of images is restricted to the shapes enclosed by boundaries that are straight lines. This is because the only mirror that gives a point image for point source is a plane mirror. Even for polygonal shapes, the images can be uniquely specified in the two dimensional space only if the internal angle at each vertex of the polygon is a sub-multiple of pie. Thus, this method is restricted to rectangles and some types of triangular shapes.

The Green's function for various geometries, appear as double infinite summations. In the numerical computations of the impedance matrix elements, the corresponding Green's function is integrated over the port widths. The order of integrations and summations can be interchanged. The integrals involved were carried out analytically to get the impedance matrix elements for each of the geometries considered in this thesis.

Green's function [7,8] and corresponding impedance matrix elements for the basic figures used in the thesis are as follows:-

(a) A Rectangle:

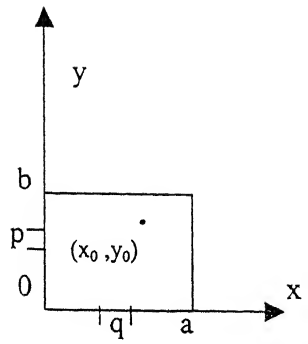

Figure 4.2 Geometry and port locations for a rectangular planar segment

The Green's function for the rectangle shown in figure 4.2 with sides of rectangle oriented along x and y-axis is given as: -

$$G(x,y\,|\,x_o,y_o)=\frac{j\omega\mu d}{ab}\sum_{m=0}^{\infty}\sum_{n=0}^{\infty}\frac{\sigma_m\sigma_n\cos(k_x x_o)\cos(k_y y_o)\cos(k_x x\ )\cos(k_y y\ )}{k_x^2+k_y^2-k^2}, \qquad (4.3)$$

and the impedance matrix element Z_{pq} is written in the form: -

$$Z_{pq}=\frac{j\omega\mu d}{ab}\sum_{m=0}^{\infty}\sum_{n=0}^{\infty}\frac{\sigma_m\sigma_n\phi_{mn}(x_p,y_p)\phi_{mn}(x_q,y_q)}{k_x^2+k_y^2-k^2}. \qquad (4.4)$$

Where σ_i = {1 if i = 0 and 2 otherwise}, $k_x = m\pi/a$, $k_y = n\pi/b$ and $k^2=\omega^2\mu\varepsilon_o\varepsilon_r(1-j\delta)$

and ϕ_{mn} , for ports oriented along the y direction, is

$$\phi_{mn}(x,y) = \cos(k_x x)\cos(k_y y)\,\mathrm{sinc}(k_y W/2), \qquad (4.5)$$

and ϕ_{mn} , for ports oriented along the x direction, is

$$\phi_{mn}(x,y) = \cos(k_x x)\cos(k_y y)\,\mathrm{sinc}(k_x W/2). \qquad (4.6)$$

Where δ is the loss tangent of the dielectric, a is the rectangle's length, b is its width, d is the substrate height, points (x_p, y_p) and (x_q, y_q) denotes the location of ports p and q and W, width of the port.

The doubly infinite series of equation 4.3 can be reduced to a singly infinite series by summing the inner sum [19]. The choice of summation n or m depends on the relative locations of ports p and q and also the aspect ratio of the rectangular segment.

(b) A right-angled isosceles triangle.

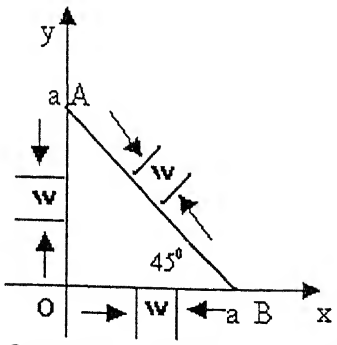

Figure 4.3 Geometry and port locations for a right-angled isosceles triangle planar segment

The Green's function for the right-angled isosceles triangle, with sides of triangle oriented along x and y-axis as shown in figure 4.3, is given as: -

$$G(x,y \mid x_o,y_o) = \frac{j\omega\mu d}{2}\sum_{m=0}^{\infty}\sum_{n=0}^{\infty}\frac{\sigma_m\sigma_n T(x_o,y_o)\,T(x,y)}{(m^2+n^2)\pi^2 - a^2k^2}, \tag{4.7}$$

where

$$T(x,y) = \cos\frac{m\pi x}{a}\cos\frac{n\pi y}{a} + (-1)^{m+n}\cos\frac{n\pi x}{a}\cos\frac{m\pi y}{a}, \tag{4.8}$$

and the impedance matrix element Z_{pq} is written as

$$Z_{pq} = \frac{j\omega\mu d}{2W_pW_q}\sum_{m=0}^{\infty}\sum_{n=0}^{\infty}\frac{\sigma_m\sigma_n I_T(p)I_T(q)}{(m^2+n^2)\pi^2 - a^2k^2}. \tag{4.9}$$

Where I_T(p) and I_T(q) are integrals of the function T(x,y) as defined above in (4.8), over the widths W of the respective ports. With reference to figure 4.3 the following expressions apply

For the ports along the side OA

$$\frac{I_T(p)}{W_p} = \cos\frac{m\pi x_p}{a}\cos\frac{n\pi y_p}{a}\sin c\frac{n\pi w_p}{2a} + (-1)^{m+n}\cos\frac{n\pi x_p}{a}\cos\frac{m\pi y_p}{a}\sin c\frac{m\pi w_p}{2a}. \tag{4.10}$$

For the ports along the side OB

$$\frac{I_T(p)}{W_p} = \cos\frac{n\pi y_p}{a}\cos\frac{m\pi x_p}{a}\sin c\frac{m\pi w_p}{2a} + (-1)^{m+n}\cos\frac{m\pi y_p}{a}\cos\frac{n\pi x_p}{a}\sin c\frac{n\pi w_p}{2a} \quad (4.11)$$

For the ports along the side AB

$$\frac{I_T(p)}{W_p} = (-1)^n\{\cos\frac{(m+n)\pi x_p}{a}\sin c\frac{(m+n)\pi w_p}{2\sqrt{2}a} + \cos\frac{(m-n)\pi x_p}{a}\sin c\frac{(m-n)\pi w_p}{2\sqrt{2}a}\} \quad (4.12)$$

(b) A 30°- 60° right –angled triangle:

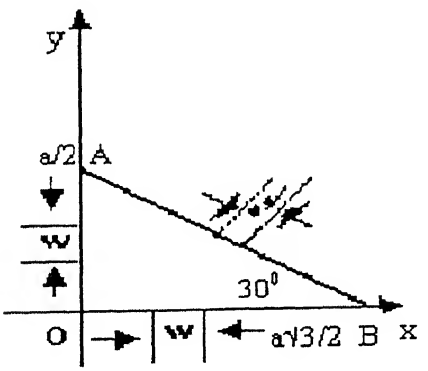

Figure 4.4 Geometry and port locations for a 30°- 60° right-angled triangle planar segment

The Green's function for the 30°- 60° right-angled triangle, with sides of triangle oriented along x and y-axis as shown in figure 4.4, is

$$G(x,y|x_o,y_o) = 8j\omega\mu d\sum_{m=-\infty}^{\infty}\sum_{n=-\infty}^{\infty}\frac{T_1(x_o,y_o)\,T_1(x,y)}{16\sqrt{3}\pi^2(m^2+mn+n^2)-9\sqrt{3}a^2k^2}, \quad (4.13)$$

where

$$T_1(x,y) = (-1)^l \cos\frac{2\pi l x}{\sqrt{3}a}\cos\frac{2\pi(m-n)y}{3a} + (-1)^m \cos\frac{2\pi m x}{\sqrt{3}a}\cos\frac{2\pi(n-l)y}{3a} + (-1)^n \cos\frac{2\pi n x}{\sqrt{3}a}\cos\frac{2\pi(l-m)y}{3a}, \quad (4\ 14)$$

with condition that $l = -(m+n)$.

The impedance matrix element Zpq is written as

$$Z_{pq} = \frac{8J\omega\mu d}{W_p W_q}\sum_{m=-\infty}^{\infty}\sum_{n=-\infty}^{\infty}\frac{I_{T1}(p)I_{T1}(q)}{16\sqrt{3}\pi^2(m^2+mn+n^2)-9\sqrt{3}a^2k^2}, \quad (4.15)$$

where $I_{T1}(p)$ and $I_{T1}(q)$ are integrals of the function $T_l(x, y)$ as defined above , over the widths W of the respective ports. With reference to figure 4.4 the following expressions apply

For the ports along the side OA

$$\frac{I_{T1}(p)}{W_p} = (-1)^l \cos\frac{2\pi l x_p}{\sqrt{3}a}\cos\frac{2\pi(m-n)y_p}{3a}\operatorname{sinc}\frac{\pi(m-n)W_p}{3a} + (-1)^m \cos\frac{2\pi m x_p}{\sqrt{3}a}\cos\frac{2\pi(n-l)y_p}{3a}\operatorname{sinc}\frac{\pi(n-l)W_p}{3a} + (-1)^n \cos\frac{2\pi n x_p}{\sqrt{3}a}\cos\frac{2\pi(l-m)y_p}{3a}\operatorname{sinc}\frac{\pi(l-m)W_p}{3a} \quad (4.16)$$

For the ports along the side OB

$$\frac{I_{T1}(p)}{W_p} = (-1)^l \cos\frac{2\pi(m-n)y_p}{3a}\cos\frac{2\pi l x_p}{\sqrt{3}a}\operatorname{sinc}\frac{\pi l W_p}{\sqrt{3}a} + (-1)^m \cos\frac{2\pi(n-l)y_p}{3a}\cos\frac{2\pi m x_p}{\sqrt{3}a}\operatorname{sinc}\frac{\pi m W_p}{\sqrt{3}a} + (-1)^n \cos\frac{2\pi(l-m)y_p}{3a}\cos\frac{2\pi n x_p}{\sqrt{3}a}\operatorname{sinc}\frac{\pi n W_p}{\sqrt{3}a} \quad (4.17)$$

For the ports along the side AB

$$\frac{I_{T1}(p)}{W_p} = \cos\frac{2\pi(m-n)x_p}{a}\,\mathrm{sinc}\frac{\pi(m-n)W_p}{a} + \cos\frac{2\pi(n-l)x_p}{a}\,\mathrm{sinc}\frac{\pi(n-l)W_p}{a} + \cos\frac{2\pi(l-m)x_p}{a}\,\mathrm{sinc}\frac{\pi(l-m)W_p}{a} \quad (4.18)$$

4.4 Examples of Analysis

In this section a couple of practical structures are analyzed based on the theory of Green's function analysis and segmentation as explained in the earlier chapter. A GUI based program gives the flexibility to the user to change the parameters of the circuit interactively and see the results without actually going into the source code.

4.4.1 Two port Rectangular Resonator

As an example of a two-port network, the two-port rectangular resonator as shown in figure 4.5 is analyzed by segmentation method. The two-port rectangular resonator is divided into two segments as shown in figure 4.6, for comparison of the accuracy of computation by the segmentation method and the Green's function approach.

The resonator considered in the example is a stripline type of planar circuit whose dimensions and other electrical parameters are as follows:-

(a) Length (L) = 20.95 mm

(b) Width (W) = 7.48 mm

(c) Characteristics Impedance(Z_o) of patch = 20 Ω

(d) Width of stripline connected to ports = 2.20 mm

(e) Characteristics Impedance(Z_o) of terminations = 50 Ω

(f) Substrate Rexolite 1422 type III ε_r = 2.53

(g) Height of Substrate (2d) {ref figure 2.2} = 3.0mm

(h) Loss tangent(δ) = 0.001

The resonator dimensions and location of the ports are as shown in the figure 4.5. Rexolite 1422 type III is assumed to be the circuit material. The widths of the stripline,

which are connected to the ports, are taken such that the characteristic impedance of the line is equal to 50 Ω. In the calculations the end effect of the stripline is not considered in determining the length of line, but the width of the strip line is calculated internally as the effective width by the program.

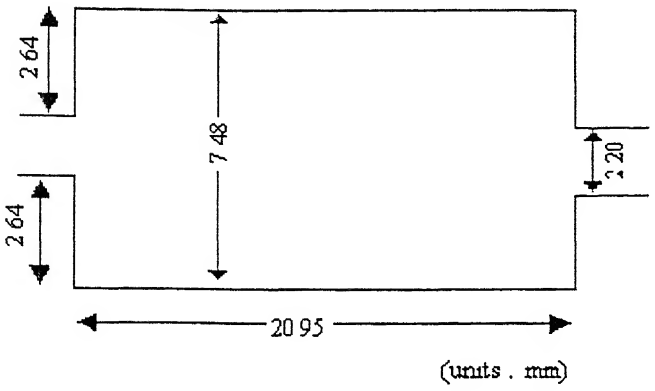

Figure 4.5 Two-port rectangular resonator

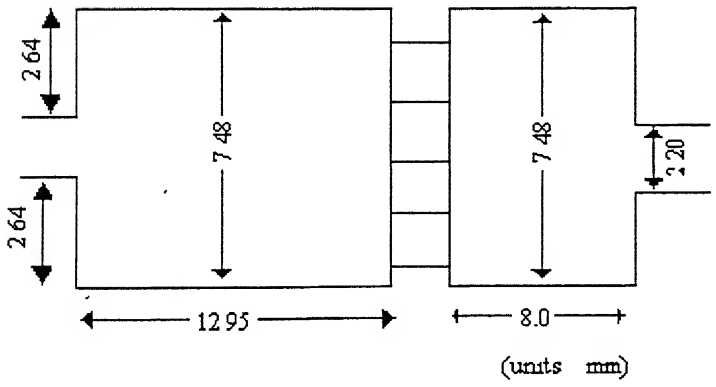

Figure 4.6 Segmented Two-port rectangular resonator with interconnections as shown.

The analysis of the above figure is done as explained in chapter 2. With the use of (4.3) to (4.6), the Z matrix elements are found which are converted to more commonly used S parameters using (2.32) and (2.34). The results are as shown in the figure 4.7 and 4.8.

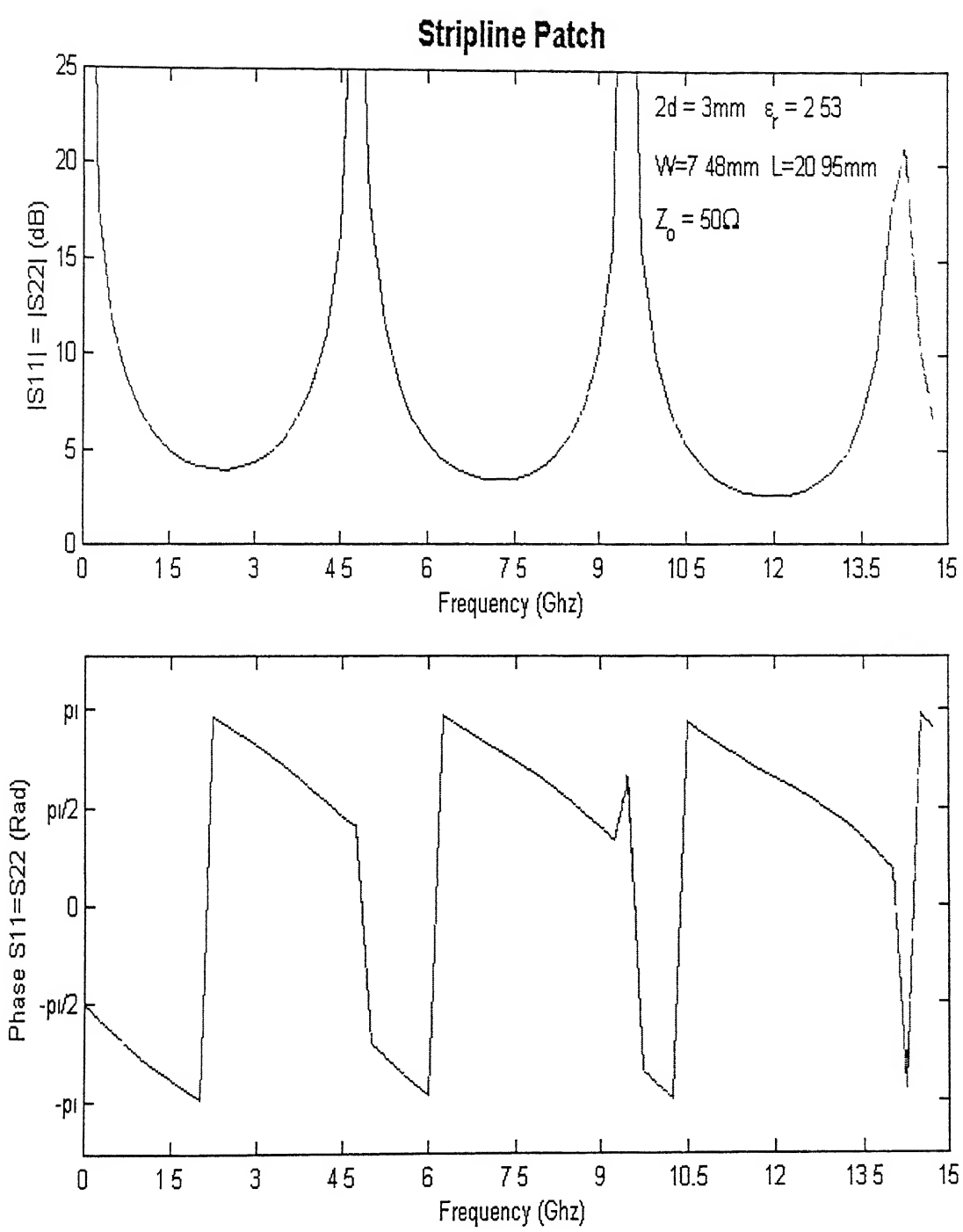

Legend

Green's function approach _____, Segmentation Method - - - - - - - -

Figure 4.7 Reflection coefficient S11 and S22 for Rectangular Resonator

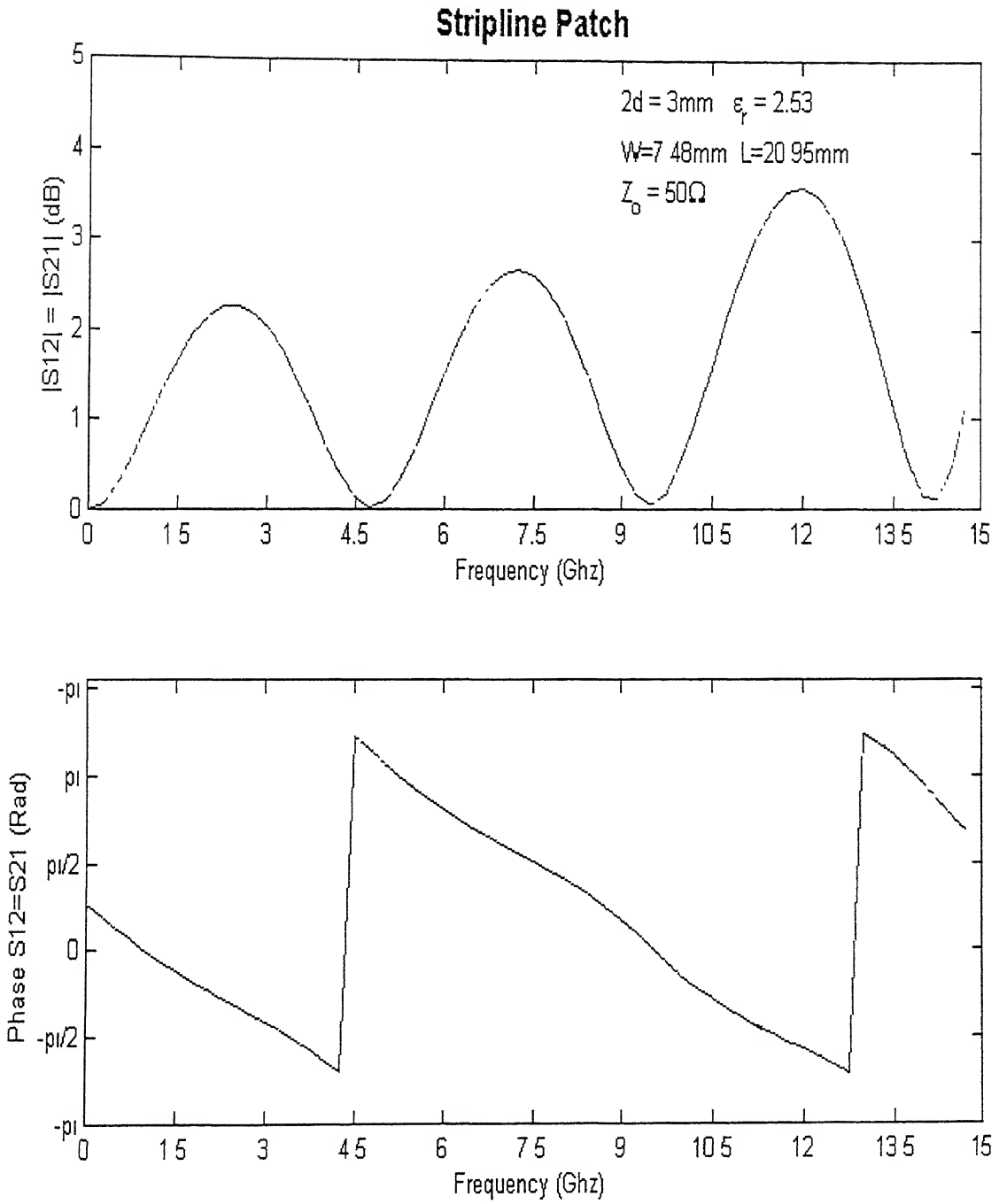

Legend

Green's function approach _____, Segmentation Method - - - - - - - -

Figure 4.8 Transfer coefficient S12 and S21 for Rectangular Resonator

4.4.2 Analysis of Result: Two-port Rectangular Resonator

The characteristics of the circuit parameters are given in terms of the scattering (S) parameters on y-axis versus frequency on x-axis. The S-parameters are an important way for representation at microwave frequencies as these can be directly related to the measurements at higher frequencies. They basically represent the relationship between incoming wave and outgoing wave at a given port. The terms of S-matrix for a two-port network are defined as follows: -

(a) S11 = Reflection coefficient at port 1.

(b) S21 = Forward transmission (transfer) coefficient from port 1 to 2.

(c) S12 = Reverse transmission (transfer) coefficient from port 2 to 1.

(d) S22 = Reflection coefficient at port 2.

For the case of reciprocal network S12 = S21 and for symmetrical network S11= S22.

The figures 4.7 and 4.8 have two sub-plots each, the top sub-plot shows the variation of amplitude and bottom sub-plot shows the variation of phase, with respect to frequency, in respect of S11=S22 and S12 =S21, respectively. The top sub-plot gives S-parameters in terms of dB, i.e. $-20\log_{10}(Sij)$. The bottom sub-plot gives phase in terms of radians. The solid line in figures 4.7 and 4.8 shows results of Green's function approach and the dashed line shows the result as calculated from the segmentation method. As evident from the figures 4.7 and 4.8 the results are almost equal for both the cases and the difference is just about 1%. The results of S11 match with the results as given in literature [3]. The various other inferences from the plot can be listed as follows: -

(a) This is a symmetrical (S11 = S22) and reciprocal (S12 = S21) network.

(b) Further as seen from the plot of S11 the maximum value is occurring near 4.7 GHz, that is the first resonance, which is actually the resonant frequency of the lowest order as calculated by theoretical formulas.

(c) Also it is evident from both the reflection coefficients and transfer coefficients that the reflection are maximum at resonant frequencies and transmission is minimum. Hence the property of resonator being a band stop filter at resonance is satisfied.

(d) From figure 4.7 it is seen that there is a phase shift of π degree at the resonant frequencies for S11 and S22.

(e) From figure 4.8 it is seen that the maximum of transfer coefficients S12 and S21 occur at 2.6 GHz and then at a gap of 4.7 GHz, the value is more at 12 GHz, due to the fact that 2d is comparable to 0.1λ beyond this frequency.

(f) From figure 4.8 it is seen that there is no phase shift in the phase of S12 and S21, and the phase changes as a smooth curve.

4.4.3 Characterization of Step Discontinuity

As an example of step discontinuity, two rectangular patches as shown in figure 4.9 make a symmetrical step in width. The discontinuity reactances (explained in chapter 3) cause the reflection coefficients on the two sides of the step to be different from their theoretical value. The step discontinuity considered is a microstrip line type of planar circuit whose dimensions and other electrical parameters are as follows: -

(a) Length (L) both segments = 10 mm

(b) Width (W) 1^{st} segment = 5.32 mm

(c) Characteristics Impedance(Z_o) 1^{st} segment = 35 Ω

(d) Width (W) 2^{nd} segment = 2.66 mm

(e) Characteristics Impedance(Z_o) 2^{nd} segment = 70 Ω

(f) Substrate Rexolite 1422 type III ε_r=2.53

(g) Height of Substrate (h) {microstrip}= 0.79mm

(h) Loss tangent(δ) of substrate = 0.001

The structure dimensions and location of the ports are as shown in the figure 4.8. In the calculations the end effect of the microstrip line is not considered in determining the length of line, as the higher order modes are present only in close vicinity of the discontinuity. But, the width of the microstrip line is calculated internally as frequency dependent effective width by the program.

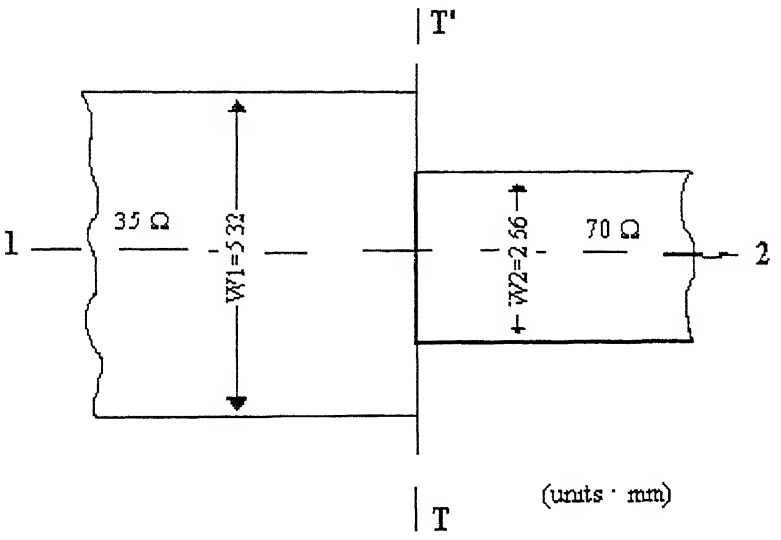

Figure 4.9 Step discontinuity at T-T' with 1:2 impedance ratio

The analysis of the step discontinuity T-T' as shown in figure 4.8 is carried out as per the procedure explained in section 3.4. Firstly, planar waveguide model for the microstrip discontinuity is calculated to account for the effect of frequency on the width and dielectric constant. Further the analysis is similar to that of the stripline case as explained in previous example. After calculating the S-parameters at the port locations the reference plane for S-parameters is shifted to the location of discontinuity. The results are as shown in the figure 4.10 and 4.11.

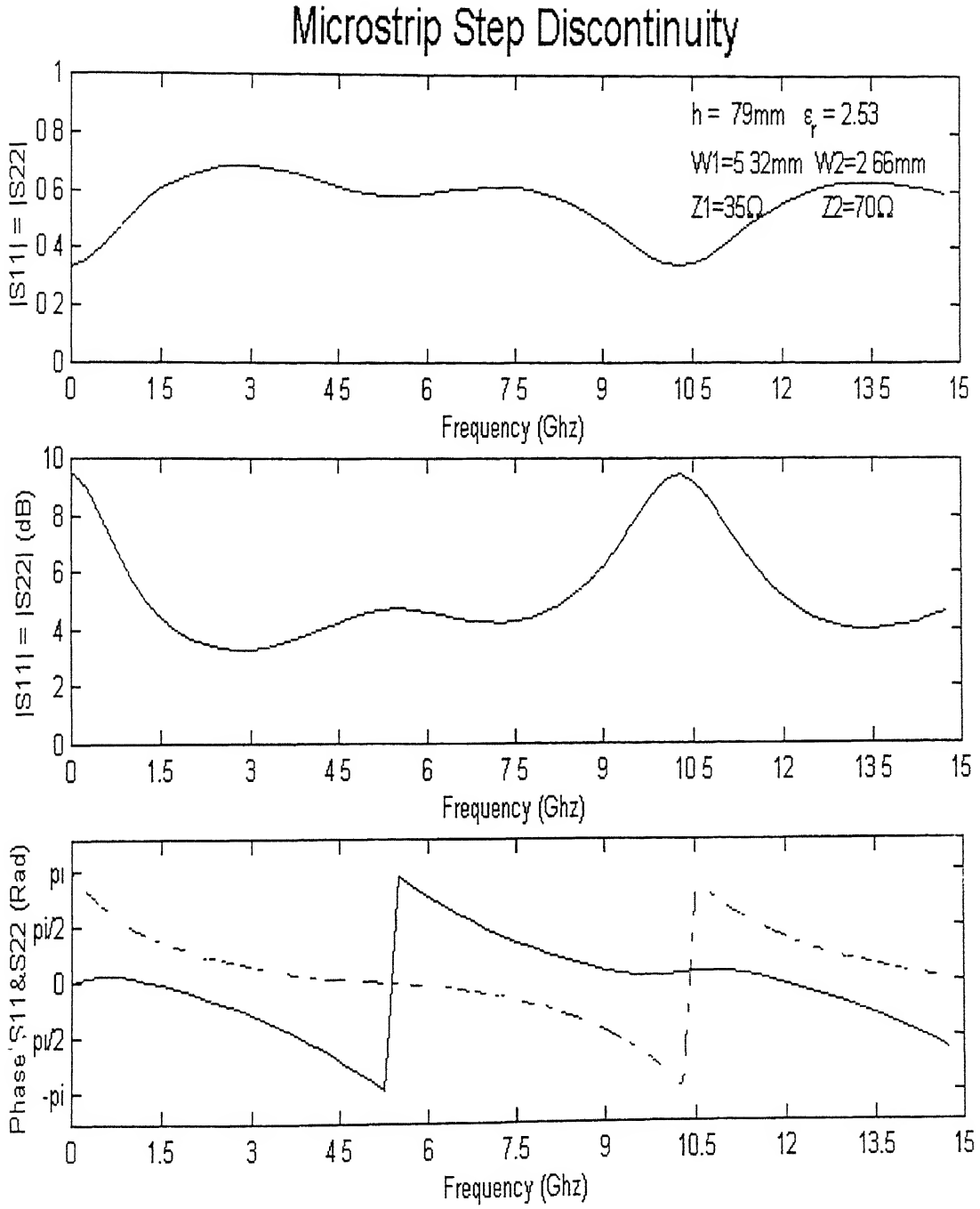

Legend

Phase S11 _____ , Phase S22 - - - - - - - -

Figure 4.10 Reflection coefficient S11 and S22 for Step Discontinuity

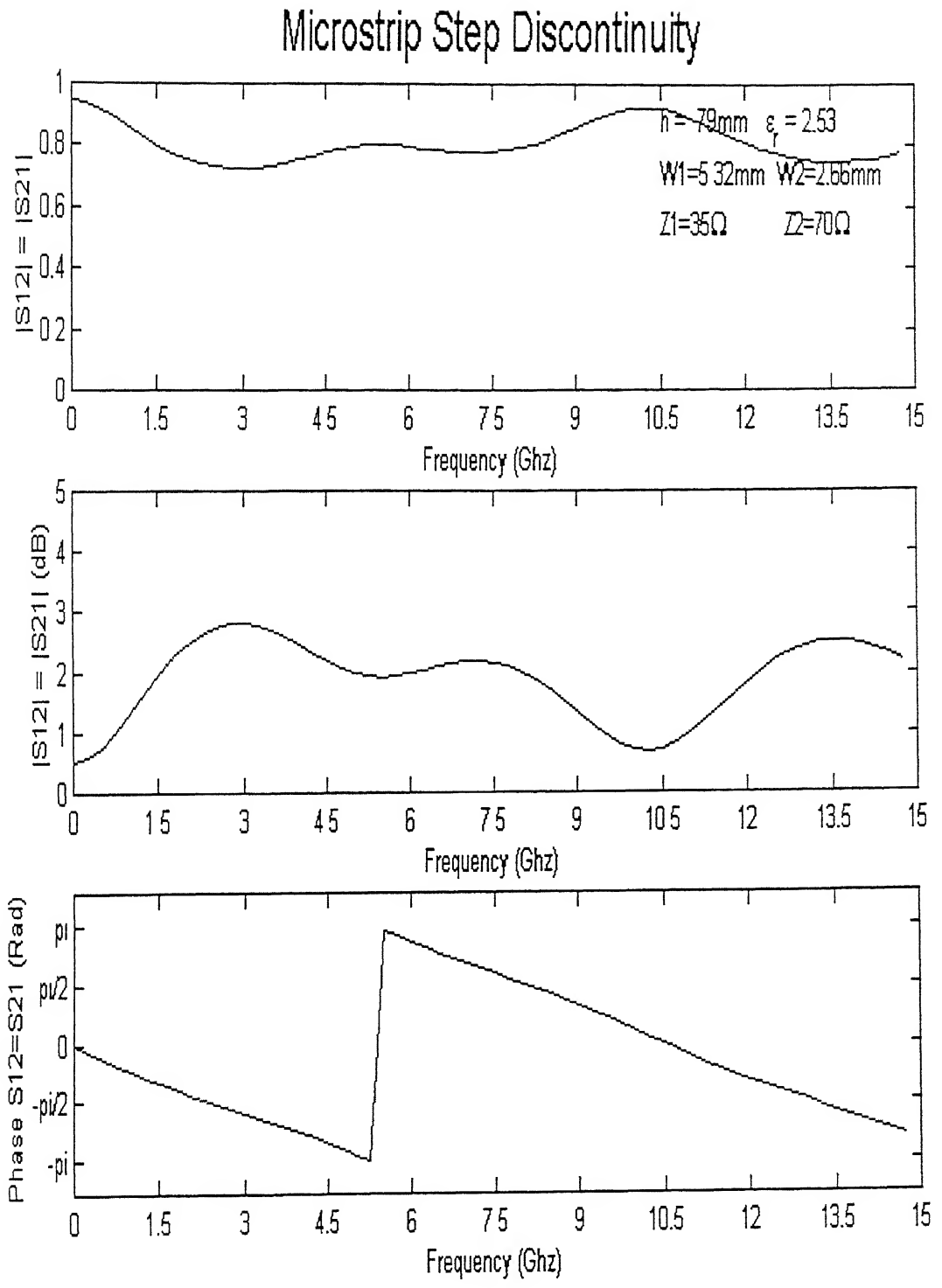

Figure 4.11 Transfer coefficient S12 and S21 for Step Discontinuity

4.4.4 Analysis of Result: Step Discontinuity

The figures 4.10 and 4.11 have three sub-plots each, the top sub-plot shows the variation of amplitude in absolute values, the middle one provides the values in dB and bottom sub-plot shows the variation of phase, with respect to frequency, in respect of S11=S22 and S12 =S21, respectively. The middle sub-plot gives S parameters in terms of dB, i.e. $-20\log_{10}(Sij)$. The bottom sub-plot gives phase in terms of radians. The solid line in figure 4.10 show results of phase of S11 and the dashed line show the phase of S22. The results of S11 match with the results as given in literature [17]. The various other inferences from the plot can be listed as follows: -

(a) This is a reciprocal (S12 = S21) network but not symmetrical as there is difference of π in the phase of S11 and S22.

(b) From figure 4.10 it is seen that the reflection coefficient which should be 1/3 for the discontinuity ratio of 1:2 by theoretical formulas, is 1/3 at low frequencies but varies at higher frequencies.

(c) The value of S11 and is around 0.6 for most of the frequencies.

(d) From figure 4.11 it is seen that the transmission coefficient values are between 0.8 to 0.9 for the entire spectrum, in accordance with the results in literature [14].

(e) From figure 4.11 it is seen that there is no phase shift in the phase of S12 and S21, and the phase changes as a smooth curve.

4.4.5 Characterization of Double-Step Discontinuity

Though there was no particular reference found in the literature surveyed regarding a double step discontinuity. But, an example of double-step discontinuity is also undertaken, three rectangular patches as shown in figure 4.12 making two symmetrical steps in width is considered. The discontinuity reactances (explained in

chapter 3) cause the reflection coefficients on the two sides of the both the steps to be different from their theoretical value. The step discontinuity considered is a microstrip line type of planar circuit whose dimensions and other electrical parameters are as follows: -

(a) Length (L), all segments = 10 mm

(b) Width (W) 1st segment = 5.32 mm

(c) Characteristics Impedance(Z_o) 1st segment = 35 Ω

(d) Width (W) 2nd segment = 3.75 mm

(e) Characteristics Impedance(Z_o) 2nd segment = 50 Ω

(f) Width (W) 3rd segment = 2.66 mm

(g) Characteristics Impedance(Z_o) 3rd segment = 70 Ω

(h) Substrate Rexolite 1422 type III ε_r=2.53

(i) Height of Substrate (h) {microstrip}= 0.79mm

(j) Loss tangent(δ) of substrate = 0.001

The structure dimensions and location of the ports are as shown in the figure 4.12. In the calculations the end effect of the microstrip line is not considered in determining the length of line, as the higher order modes are present only in close vicinity of the discontinuity. But the effective width of the microstrip line is calculated.

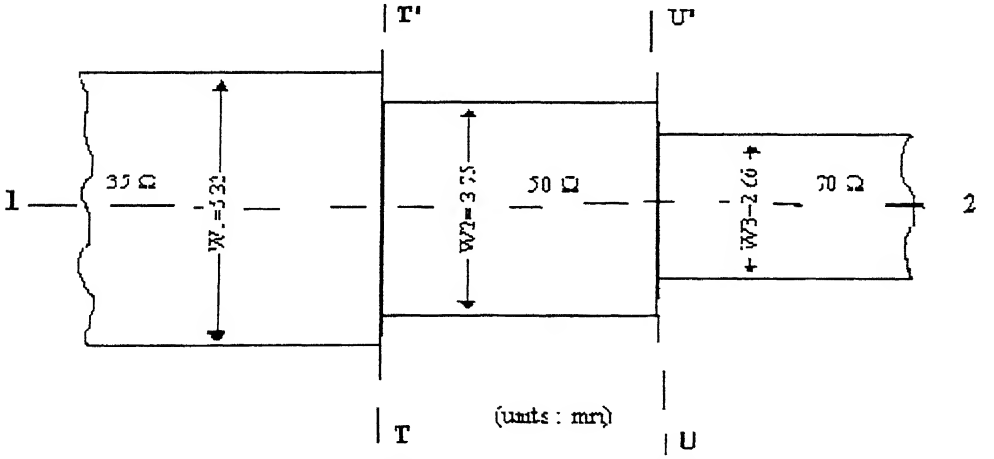

Figure 4.12 Double Step discontinuity at T-T' and U-U'

The analysis of the above figure 4.12 is done as explained in previous example of step discontinuity. The results are as shown in the figure 4.13 and 4.14.

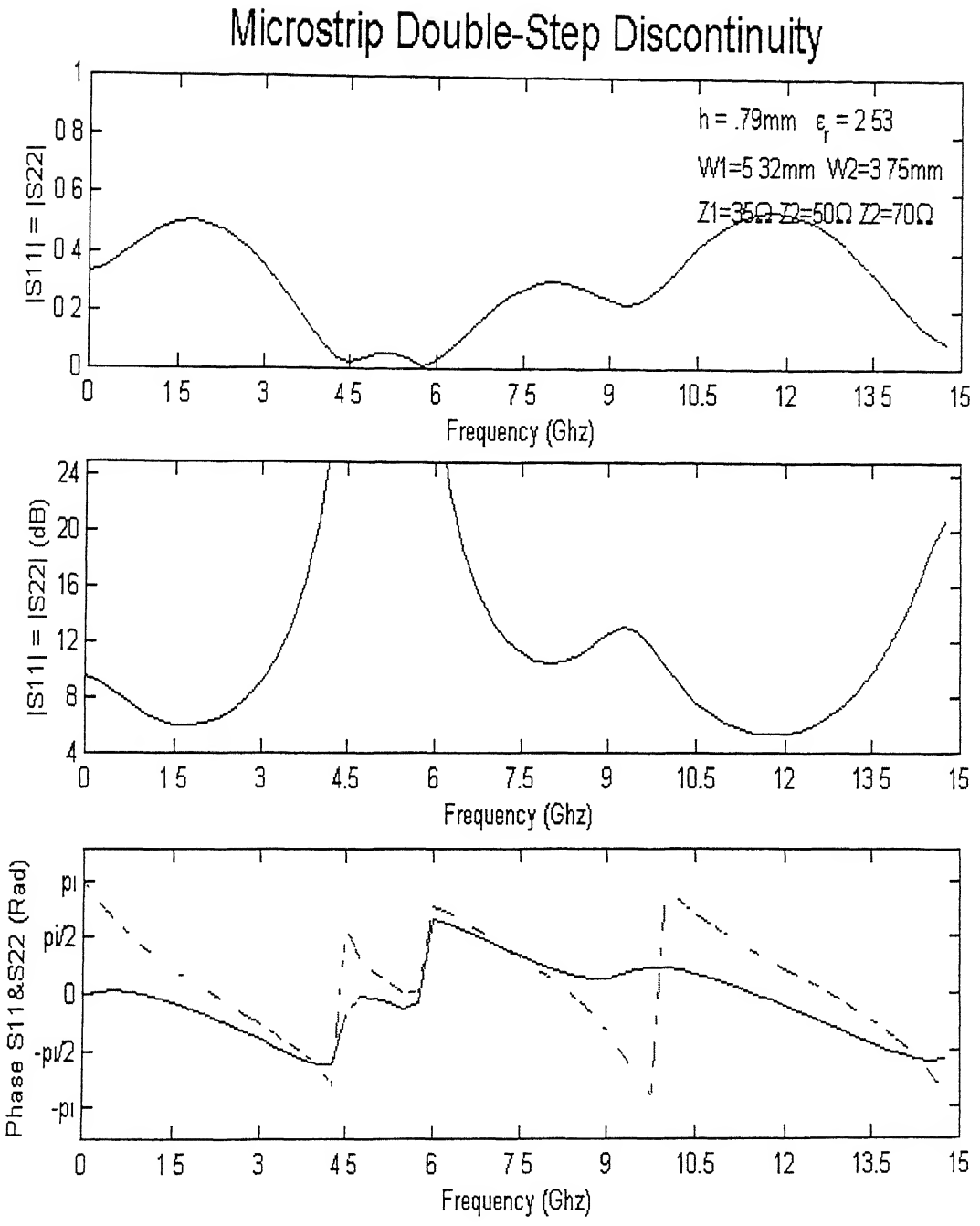

Legend

Phase S11 _____ , Phase S22 - - - - - - - -

Figure 4.13 Reflection coefficient S11 and S22 for Double Step Discontinuity

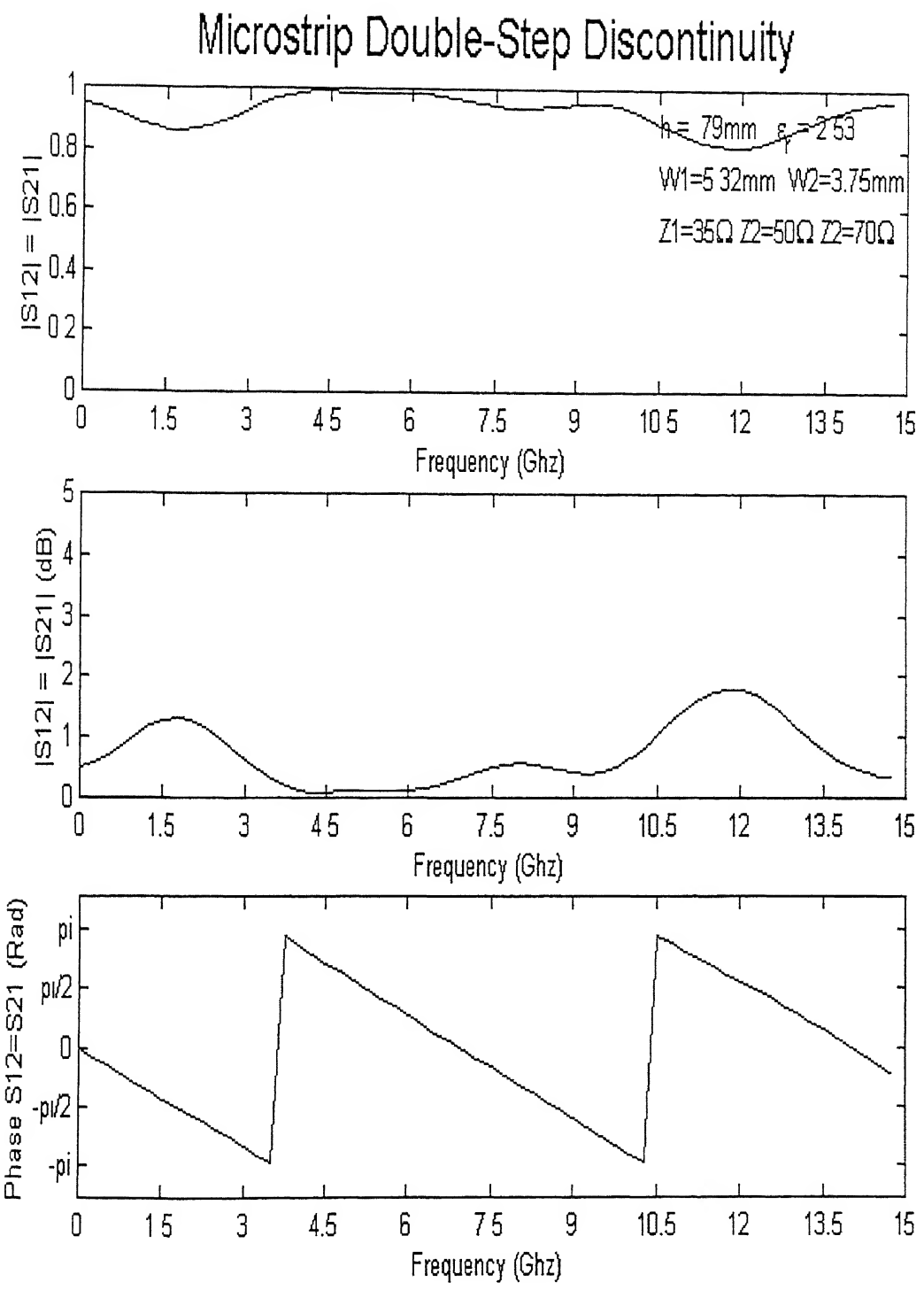

Figure 4.14 Transfer coefficient S12 and S21 for Double Step Discontinuity

4.4.6 Analysis of Result: Double Step Discontinuity

The figures 4.13 and 4.14 have three sub-plots each, the top sub-plot shows the variation of amplitude in absolute values, the middle one provides the values in dB and bottom sub-plot shows the variation of phase, with respect to frequency in respect of S11=S22 and S12=S21, respectively. The middle sub-plot gives S-parameters in terms of dB, i.e. $-20\log_{10}(S_{ij})$. The bottom sub-plot gives phase in terms of radians. The solid line in figure 4.13 show results of phase of S11 and the dashed line show the phase of S22. The various other inferences from the plot can be listed as follows: -

(a) This is a reciprocal (S12 = S21) network but not symmetrical as there is difference in the phase of S11 and S22.

(b) If we compare the results of the step discontinuity with double step discontinuity in respect of reflection coefficient we find the reflection coefficient to be better in the double step than the single step case by 4-5 dB, in all of the frequency range other than 4.5 to 6 GHz.

(c) From the figure 4.13 we see that there is no reflections around 5 GHz, which is due to the fact that length of central segment becomes $\lambda/4$ and the center segment acts as impedance transformer.

(d) From figure 4.14 it is seen that there is no phase shift in the phase of S12 and S21, and the phase changes as a smooth curve.

(e) From figure 4.14 it is seen that the transmission coefficients are better then 2 dB for the frequency range under consideration.

CHAPTER 5

SUMMARY AND CONCLUSIONS

5.1 Summary

Feasibility of developing a graphical user interface based computer program for microwave circuit design has been studied. Although there are a number of commercially available softwares for the purpose but due to high costs, copyright restrictions and complexity in usage of these softwares, these are not of much use in academic environment. Moreover for the students of electromagnetics and microwave engineering there is more of a requirement to learn the theory behind such design, and then develop and analyze the circuit. Keeping in view the above requirement a code is written to develop the framework of the graphical user interface, which is then integrated with the computation method of planar circuit analysis for design and analysis of the microwave circuit elements.

Generally the microwave circuits are characterized into three principal categories of electric circuits. These categories consist of lumped elements, zero-dimensional; the transmission line type of distributed circuitry, one-dimensional; waveguide type, three-dimensional. Complimentary to the above stated categories is a fourth category, which can be termed as a two-dimensional circuit. The planar circuit analysis is based on the concept of modeling of microwave circuits on the two-dimensional model, where two dimensions of the circuits are comparable to the wavelength, but the third dimension is a negligible fraction of the wavelength. Although planar circuit model provides an approximate analysis but it gives considerable accuracy over the traditional transmission line model of microstrip circuits.

In planar circuit analysis the electromagnetic field is considered invariant in one of the dimensions and hence the wave equation dealt with is two-dimensional Helmholtz equation, which can be solved using Green's function approach and the

regular geometrical figures has been considered. For a general case of n–port planar circuit impedance matrix elements have been defined in terms of the integration of the Green's function over the width of the ports under consideration. From these Z-matrix elements the more commonly used S-matrix elements are calculated.

The planar circuit approach is then extended by introducing segmentation of planar elements. As the Green's functions are known for only a limited number of structural shapes, a more complicated shape can be segmented into elementary shapes for which the impedance matrix can be calculated. Then the common ports are connected to form the original circuit, and overall Z-matrix of the complicated segment is found. Another complimentary method is the desegmentation method. This technique is applicable for the structure, which can be analyzed by Green's function method or segmentation method if a simple element is added to it.

The discontinuities are inherent part of any microwave integrated circuitry, and have considerable effect in the performance of the circuit. Hence, the characterisation of discontinuities is a major requirement for the design of microwave circuit. The characterisation of discontinuities in microstrip line type of planar circuits has been carried out with the help of planar circuit model and use of segmentation method. With the help of examples using Green's function approach and segmentation method results are generated for simple shapes and discontinuities and are illustrated as S-parameter versus frequency graphs.

5.2 Conclusions

It has been shown that a simple graphical user interface for microwave circuit design can be developed using MATLAB program, which can be altered according to the need. Integration of various types of computational techniques can be incorporated in this software. As an example, planar circuit analysis method is integrated into the software. Planar circuit analysis based on Green's function approach is incorporated to analyze some simple geometry. Segmentation and desegmentation approach as extension of Green's function approach is also incorporated to analyze complicated geometry, which can be formed by simple geometry. For checking the utility of the software developed a couple of examples are considered. With the help of example of

a simple rectangular patch, comparison of Green's function approach and calculations by segmentation method was made in respect of S-parameters as a function of frequency. The differences between results of S-parameters were found by the two methods was just about 1%, which validates the segmentation procedure used. Two more examples were taken to analyze the effect of discontinuity as dependent on frequency.

5.3 Scope for further work

The graphical user interface can be further improved to take inputs as drawing of microwave circuit elements with actual dimensions, and to provide outputs based on the smith chart. These are purely software-related aspects, and can be incorporated by using the available software tools. In the thesis using planar circuit analysis, two-port networks have been analyzed the same approach can be extended for analysis of four-port and N-port networks. Also in the thesis the characterisation of the discontinuities in terms S-parameters has been done, further work can be done to analyze discontinuities by providing compensation with the help of segmentation and desegmentation method, and effects studied.

References

[1] Takanoro Okoshi and Tanroku Miyoshi, "The planar circuit –An approach to microwave integrated circuitry," IEEE Trans. Microwave Theory Tech., Vol.MTT-20, No.4, PP 245-252, April 1972.

[2] Takanoro Okoshi and Tanroku Miyoshi, "Analysis of microwave planar circuits," Electron. commun. Japan., Vol.55-B, no.8, pp.24-31, 1972.

[3] T. Okoshi and T. Takeuchi, " Analysis of planar circuits by planar segmentation method," Electron. commun. Japan, Vol.58-B, no.8, pp.71-79, Aug.1975.

[4] T.Okoshi, Y.Uehara and T. Takeuchi, "The segmentation method – An approach to the Analysis of Microwave planar circuits," IEEE Trans. Microwave Theory Tech., Vol. MTT-24, PP 662-668, Oct. 1976.

[5] R.Chadha and K.C. Gupta, " Segmentation method using impedance matrices for analysis of planar Microwave circuits," IEEE Trans. Microwave Theory Tech., Vol. MTT-29, PP 71-74, Jan. 1981.

[6] K.C. Gupta, R.Garg, and R. Chadha, Computer-Aided Design of Microwave Circuits, Artech House, Dedham, MA, 1981.

[7] R.Chadha and K.C. Gupta, " Green's functions for triangular segments in microwave planar circuits," IEEE Trans. Microwave Theory Tech., Vol. MTT-28, PP 1139-1143, Oct. 1980.

[8] R.Chadha and K.C. Gupta, " Green's functions for circular sectors, annular rings and annular sectors in planar microwave circuits," IEEE Trans. Microwave Theory Tech., Vol. MTT-29, PP 68-71, Jan. 1981.

[9] P.C. Sharma and K.C. Gupta, " Desegmentation method for the analysis of two-dimensional Microwave circuits," IEEE Trans. Microwave Theory Tech., Vol. MTT-29, PP 1094-1098, Oct. 1981.

[10] P.C. Sharma and K.C. Gupta, "An alternative procedure for implementing desegmentation method," IEEE Trans. Microwave Theory Tech., Vol. MTT-32, PP 1-4, Jan. 1984.

[11] Bharathi Bhat and Shiban Koul, Stripline-like Transmission lines for Microwave Integrated Circuits, Wiley Eastern Limited, Delhi, 1990.

[12] K.C. Gupta, R.Garg, and I.J. Bahl, Microstrip lines and Slotlines, Artech House, Dedham, MA, 1979.

[13] G. Kompa and R. Mehran, " Planar waveguide model for calculating microstrip components," Electron. Letter. , Vol. 11 pp. 459-460,1975.

[14] I.Wolff, G. Kompa and R. Mehran, "Calculation methods for microstrip discontinuities and T-junctions," Electron. Letter. , Vol. 8 pp. 177-179,1972.

[15] A. Benalla and K.C. Gupta, " Faster computation of Z-matrices for rectangular segments in planar microwave circuits," IEEE Trans. Microwave Theory Tech., Vol. MTT-34, PP 733-736, Jun. 1986.

[16] R. Sorrentino, "Planar circuits, waveguide models and segmentation method," IEEE Trans. Microwave Theory Tech., Vol. MTT-33, PP 1057-1066, Oct. 1985.

[17] R.Chadha and K.C. Gupta, " Compensation of discontinuities in planar transmission lines," IEEE Trans. Microwave Theory Tech., Vol. MTT-30, PP 2152-2156, Dec.1982

[18] K.C. Gupta and M.D. Abouzahra, " Analysis and design of four port and five port microstrip disc circuits," IEEE Trans. Microwave Theory Tech., Vol. MTT-33, PP 1422-1428, Dec.1985.

[19] T. Okoshi et al, "Planar 3-dB hybird circuit," Electron. commun. Japan., Vol.58-B, no.8, pp.80-90, Aug 1975.

[20] P.M. Morse, and H.Feshbach, Methods of Theoretical Physics, New York: McGraw Hill, 1953, ch 7.